The differentiation of prehypertrophic into hypertrophic chondrocytes drives an OA-remodeling program and IL-34 expression

Sandy van Eegher, Maria-Luisa Perez-Lozano, Indira Toillon, Damien Valour, Audrey Pigenet, Danièle Citadelle, Chantal Bourrier, Sophie Courtade-Gaïani, Laura Grégoire, Damien Cléret, et al.

The differentiation of prehypertrophic into hypertrophic chondrocytes drives an OA-remodeling program and IL-34 expression

Sandy van Eegher[1], Maria-Luisa Perez-Lozano[1], Indira Toillon[1], Damien Valour[2], Audrey Pigenet[1], Danièle Citadelle[1], Chantal Bourrier[2], Sophie Courtade-Gaïani[2], Laura Grégoire[3], Damien Cléret[4], Stéphanie Malbos[1], Geoffroy Nourissat[1,5], Alain Sautet[6], Marie-Hélène Lafage-Proust[4], Philippe Pastoureau[2], Gaëlle Rolland-Valognes[2], Frédéric De Ceuninck[2], Francis Berenbaum[1, 7,*], Xavier Houard[1]

[1] Sorbonne Université, INSERM, Centre de Recherche Saint-Antoine (CRSA), F-75012 Paris, France.
[2] Servier Research Institute, F-78290 Croissy-sur-Seine, France.
[3] Soladis**,** 94 Rue Saint-Lazare, F-75009 Paris, France.
[4] Université de Lyon - Université Jean Monnet, INSERM U1059, Faculté de Médecine, F-42270 Saint-Priest en Jarez, France.
[5] Clinique Maussins-Nollet, Ramsay Générale de Santé, F-75019 Paris, France.
[6] Department of Orthopaedic Surgery and Traumatology, APHP Saint-Antoine Hospital, F-75012 Paris, France.
[7] Sorbonne Université, INSERM CRSA, AP-HP Hopital Saint Antoine, Paris,

* Address for correspondence:

Francis Berenbaum, MD, PhD.
Centre de Recherche Saint-Antoine,
184 rue du Faubourg Saint-Antoine
F-75012 Paris
France
Email: francis.berenbaum@aphp.fr

Running title: Prehypertrophic chondrocytes in osteoarthritis

Word count: 4003

Abstract

Objectives. We hypothesize that chondrocytes from the deepest articular cartilage layer are pivotal in maintaining cartilage integrity and that the modification of their prehypertrophic phenotype to a hypertrophic phenotype will drive cartilage degradation in osteoarthritis.

Design. Murine immature articular chondrocytes (iMACs) were successively cultured into three different culture media to induce a progressive hypertrophic differentiation. Chondrocyte were phenotypically characterized by whole-genome microarray analysis. The expression of IL-34 and its receptors PTPRZ1 and CSF1R in chondrocytes and in human osteoarthritis tissues was assessed by RT-qPCR, ELISA and immunohistochemistry. The expression of bone remodeling and angiogenesis factors and the cell response to IL-1β and IL-34 were investigated by RT-qPCR and ELISA.

Results. Whole-genome microarray analysis showed that iMACs, prehypertrophic and hypertrophic chondrocytes each displayed a specific phenotype. IL-1β induced a stronger catabolic effect in prehypertrophic chondrocytes than in iMACs. Hypertrophic differentiation of prehypertrophic chondrocytes increased Bmp-2 (95%CI [0.78;1.98]), Bmp-4 (95%CI [0.89;1.59]), Cxcl12 (95%CI [2.19;5.41]), CCL2 (95%CI [3.59;11.86]), Mmp3 (95%CI [10.29;32.14]) and Vegf mRNA expression (95%CI [0.20;1.74]). Microarray analysis identified IL-34, PTPRZ1 and CSFR1 as being strongly overexpressed in hypertrophic chondrocytes. IL-34 was released by human osteoarthritis cartilage; its receptors were expressed in human osteoarthritis tissues. IL-34 stimulated CCL2 and MMP13 in osteoblasts and hypertrophic chondrocytes but not in iMACs or prehypertrophic chondrocytes.

Conclusion. Our results identify prehypertrophic chondrocytes as being potentially pivotal in the control of cartilage and subchondral bone integrity. Their differentiation into

hypertrophic chondrocytes initiates a remodeling program in which IL-34 may be involved.

Keywords: Osteoarthritis, prehypertrophic chondrocytes, osteochondral junction, chondrocyte hypertrophic differentiation, IL-34

Introduction

Osteoarthritis (OA) is characterized by the irreversible degradation of cartilage, which is associated with a pathological remodeling of the subchondral bone, including sclerosis and osteophyte formation. Cartilage degradation mainly results from the proteolysis of the cartilage extracellular matrix by chondrocyte-secreted proteases [1]. The degradation observed in the deep zone of articular cartilage is explained by an endochondral ossification-like process at the cartilage/bone interface [2-4], which involves the hypertrophic differentiation of chondrocytes, the calcification and the vascularization of the extracellular matrix followed by the replacement of cartilage with bone.

While chondrocytes are the unique cell type present within cartilage, different chondrocyte phenotypes exist, depending on the type of cartilage and on the chondrocyte localization within cartilage. Articular cartilage is organized in different layers from the surface until the subchondral bone. The phenotype of chondrocytes differs upon the layer considered [5]. Chondrocytes from the deepest articular cartilage layer of non-calcified cartilage display an intermediate phenotype between that of the chondrocytes of the surface layers and that of the chondrocytes found in the calcified cartilage, which are hypertrophic. They indeed express molecules that characterize both surface layer chondrocytes and hypertrophic chondrocytes, including type II and type X collagens [6-8]. They also express Ihh and osteomodulin as prehypertrophic chondrocytes from the growth plate cartilage [9-12].

Cartilage degradation in OA results in chondrocyte phenotypic modifications. We hypothesize that the chondrocytes from the deepest articular cartilage layer play a crucial role in maintaining cartilage integrity and that the modification of their prehypertrophic phenotype to a hypertrophic phenotype will drive cartilage degradation in OA. In the present study, we developed a model of progressive differentiation of murine immature

articular chondrocytes (iMACs) into hypertrophic chondrocytes, and this model includes an intermediate prehypertrophic state. Here, we show that the differentiation of prehypertrophic chondrocytes into hypertrophic chondrocytes shifts chondrocytes towards an OA-inducing phenotype. This phenotype is associated with an increased expression of IL-34, a recently discovered cytokine that could be involved in both cartilage and bone integrity.

Materials and methods

See supplementary information for detailed Material and methods.

Collection of osteoarthritis human samples

Human OA knee explants (n=33) obtained from patients undergoing total knee joint replacement surgery were dissected, as described [13].

Immunohistochemistry

Immunohistochemistry was performed with a mouse monoclonal antibody against PTPRZ1 (clone 12/RPTPb, BD Transduction Laboratories; dilution 1:50) and a rabbit polyclonal antibody against CSF-1R (H-300, Santa Cruz Biotechnology; dilution 1:50) as the primary antibodies. The R.T.U. Vectastain kit (Vector) was used for detection, followed by counterstaining with Mayer's hematoxylin. Irrelevant control antibodies (Dako) were incubated at the same concentration to assess nonspecific staining.

Primary culture of murine osteoblasts and articular chondrocytes

Osteoblasts and iMACs were isolated and cultured, as described in [14-16] and supplementary information. Prehypertrophic chondrocytes were obtained by culturing iMACs for 28 days in culture medium 2 (DMEM/HAM-F12 medium supplemented with fetal calf serum (5%), penicillin (100 U/mL), streptomycin (100 µg/mL), L-glutamine (4 mM), ascorbic acid (40 µg/mL), insulin-transferrin-sodium selenite (1%) and triiodo-L-thyronine (50 ng/mL)). Chondrocytes were further cultured for 42 days in medium 2 supplemented with β-glycerophosphate (10 mM), retinoic acid (100 nM) and 1α,25-dihydroxyvitamin D_3 (10 nM) (Medium 3) to obtain hypertrophic chondrocytes. All

cultures were performed in standard conditions with the exception of the last differentiation step, performed in 3% CO_2/95% air. At the end of the culture, cells were serum-starved for 24 hours and stimulated by recombinant human IL-1β (1 ng/mL) or murine IL-34 (3, 30 and 100 ng/mL) for 24 hours. Conditioned media were kept, centrifuged and stored at -20°C. Cells were either fixed in 3.7% paraformaldehyde (PFA) or used for mRNA or protein extraction.

The experimental design for the cell culture study is shown in Fig. S1.

Primary culture of human articular chondrocytes

Human chondrocytes were isolated from the less damaged areas of OA cartilage from patients who underwent total knee arthroplasty. Their hypertrophic differentiation was performed according to Yahara *et al.* [17].

Microarray analysis

mRNA expression profiling was performed using SurePrint G3 Mouse Gene Expression v2 8x60K Microarray (G4852B, Agilent Technologies) and SurePrint Mouse miRNA Microarray Kit v21 8x60K (G4859C, Agilent Technologies). For mRNA profiling, probe labeling and 60 mer-oligonucleotide microarray hybridization were performed according to the manufacturer's instructions [18]. An Agilent scanner and Feature Extraction 11.5.1.1 software (Agilent Technologies) were used to obtain the raw microarray data for both analyses.

Statistical analysis

We used repeated measures one-way ANOVA to compare iMACs, prehypertrophic and hypertrophic chondrocytes. Paired t-tests were used to compare prehypertrophic to hypertrophic chondrocyte gene expression observations and gene or protein comparison in OA patients. For the IL-1β and IL-34 stimulation study, we used Dunnett's post hoc test. The analyses were performed using GraphPad Prism7 (GraphPad Software Inc., San Diego, CA, USA).

Results

Model of the progressive differentiation of murine immature articular chondrocytes into prehypertrophic and hypertrophic chondrocytes

To study the consequences of the hypertrophic differentiation of chondrocytes in OA cartilage, we established an *in vitro* model of the progressive differentiation of iMACs into prehypertrophic and hypertrophic chondrocytes. iMACs displayed the typical phenotype of articular chondrocytes, characterized by the expression of Col2a1, Acan, Chm1 and Sox9 and by the almost complete absence of the expression of the hypertrophic chondrocyte markers Runx2, Osterix, MMP-13, Col10a1 and Tnap (n=6) (Fig. 1B-E and I-M). iMACs also showed weak alkaline phosphatase activity and no evidence of matrix calcification (Fig. 1O and P). Culturing the iMACs in Medium 2 then in Medium 3 induced progressive decreases in the mRNA expression of Acan, Col2a1, Sox9 and Chm1 (Fig. 1B-E). Inversely, the mRNA expression of the hypertrophic markers Runx2, Osterix, Mmp13, osteocalcin and Tnap was stimulated by culture in Medium 2 (Fig. 1I-N). The mRNA expression of Runx2, Col10a1 and osteocalcin further increased after the culture in Medium 3. Consistent with the increased mRNA expression of Tnap, the activity of alkaline phosphatase was strongly stimulated by culture in Medium 2 and Medium 3 (Fig. 1O). Significant calcification of the chondrocyte cultures was only observed when cells were cultured in Medium 3 (Fig. 1P). Cells cultured in Medium 2 expressed both iMAC and hypertrophic chondrocyte markers and did not mineralize their matrix. They also expressed the markers of prehypertrophic chondrocytes Ihh, Snorc and Osteomodulin (Fig. 1F-H). Moreover, they expressed higher mRNA levels of Snorc and Osteomodulin than iMACs and hypertrophic chondrocytes. Thus, iMACs progressively became prehypertrophic and hypertrophic after culture in Medium 2 and Medium3.

To further characterize our model of progressive hypertrophic differentiation of iMACs, the transcriptomic signatures of iMACs, prehypertrophic and hypertrophic chondrocytes were explored by high-throughput genomic methods (n=8). A two-dimensional PCA of the genes expressed revealed that all displayed globally distinct gene expression patterns (Fig. S2B), which were also confirmed by their distinct clustering patterns (Fig. S2C). Interestingly, prehypertrophic and hypertrophic chondrocytes showed a homogenous clustering pattern of gene expression, indicating that they displayed a specific molecular phenotype, different from iMAC phenotype.

The most variable genes identified by PCA (top 5000 ranked by decreasing standard deviation) accounted for 40% and 17% of the total gene expression variability in the principal component (PC) 1 and PC2 groups, respectively. Genes positively correlated with PC1 displayed an upregulation across the differentiation process. The number of genes positively correlated with PC2 was more restricted, and those were of particular interest to characterize prehypertrophic cells since they were more specifically associated with this group of cells.

The repeated spotted probes and the probes targeting the same gene were not averaged but were analyzed for similar expression. We identified 8121 differentially expressed (DE) genes (9306 DE probes, at false discovery rate (FDR)-adjusted p-value ≤ 0.05 & |Fold Change (FC)|≥ 1.3) between iMACs and hypertrophic chondrocytes (4311 and 3810 genes overexpressed in hypertrophic chondrocytes and iMACs, respectively), including markers of articular and hypertrophic chondrocytes (Table S1). The specific part of this signature represented 1467 genes (1768 DE probes, 809 and 959 overexpressed in hypertrophic chondrocytes and iMACs, respectively) (Fig. 2A). We found 6829 differentially expressed genes (7744 probes) between prehypertrophic chondrocytes and iMACs (3601 and 3228 overexpressed in prehypertrophic chondrocytes and iMACs, respectively) (Table S1),

while 1023 DE probes were specific to this contrast (540 and 483 overexpressed in prehypertrophic chondrocytes and iMACs, respectively) (Fig. 2B). Finally, 5308 genes (6220 probes) were differentially expressed between the hypertrophic and prehypertrophic chondrocytes (2970 and 2338 genes overexpressed in hypertrophic and prehypertrophic chondrocytes, respectively) (Table S1). Eight hundred nine genes (1002 DE probes) were specific to differences between hypertrophic and prehypertrophic chondrocytes (626 and 376 probes overexpressed in hypertrophic and prehypertrophic chondrocytes, respectively) (Fig. 2C). Hypertrophic chondrocytes were thus molecularly the most different from other cells.

Together, these results show that our culture model allows a progressive differentiation of the iMACs into prehypertrophic and hypertrophic chondrocytes, each displaying a specific molecular phenotype.

Prehypertrophic to hypertrophic differentiation shifts chondrocytes towards an OA-inducing phenotype

Inflammatory factors, such as IL-1β, alter the phenotype of chondrocytes that adopt OA-like catabolic features. As expected, IL-1β downregulated the expression of Col2a1 by iMACs (Padj=0.0454, 95%CI [-1.41;-0.00], n=6), whereas it strongly upregulated the mRNA expression of Il-6 (Padj=0.0016, 95%CI [1.01;2.60], n=6) and Mmp13 (Padj=0.0483, 95%CI [0.62;2.14], n=6) (Fig. 3A, C and D). IL-1β also induced a similar catabolic phenotype in prehypertrophic and hypertrophic chondrocytes (Fig. 3A-D). However, prehypertrophic chondrocytes appeared more sensitive to IL-1β than did iMACs since IL-1β led to a 2.0-fold, 4.1-fold and 1.8-fold lower expression of Col2a1, Acan and Chm1 (n=6), respectively and to a 131.7-fold higher expression of Il-6, as compared to

iMACs (Fig. 3A-C). In addition, IL-1β also stimulated the expression of Vegf and repressed those of Tsp1 and Chm1 by prehypertrophic and hypertrophic chondrocytes (n=6), while neither Vegf nor Tsp1 expression was regulated by IL-1β in iMACs (Fig. 3E-G).

To evaluate whether the shift from prehypertrophic to hypertrophic chondrocytes mimicked OA-related osteochondral remodeling, we performed analysis focused on molecular functions involved in OA (Fig. S2D). Hypertrophic chondrocytes, in contrast to prehypertrophic chondrocytes, displayed activated functions related to bone differentiation, angiogenesis and deterioration/damage of connective tissues. Accordingly, the mRNA expression of the bone remodeling factors BMP-2 (2.38-fold, 95%CI [0.78;1.98] for the difference in means), BMP-4 (2.25-fold, 95%CI [0.89;1.59] for the difference in means), CXCL12 (4.80-fold, 95%CI [2.19;5.41] for the difference in means), CCL2 (8.73-fold, 95%CI [3.59;11.86] for the difference in means) and OPG (1.75-fold, 95%CI [0.13;1.37] for the difference in means) was increased when prehypertrophic chondrocytes became hypertrophic (Fig. 3I and J). They also tended to overexpressed Rankl mRNA, as compared to prehypertrophic chondrocytes (22.5-fold, 95%CI [-4.32;47.43] for the difference in means) (Fig. 3J). Hypertrophic chondrocytes expressed more Vegf (1.97-fold, 95%CI [0.203;1.74] for the difference in means) and Mmp3 mRNAs (22.21-fold, 95%CI [10.29;32.14]) for the difference in means) and less the angiostatic factors Chm1 (-5.99-fold, 95%CI [-0.93;-0.73]) for the difference in means) and Angptl4 than prehypertrophic chondrocytes (-1.65-fold, 95%CI [-0.68;-0.10]) for the difference in means) (Fig. 3H and K). In contrast, neither Tgfβ1 nor Mpm13, Adamts4 and Adamts5 mRNAs were modulated by the switch from prehypertrophic to hypertrophic differentiation (Fig. 3H and I).

Overexpression of IL-34 by hypertrophic chondrocytes

Hypertrophic differentiation of chondrocytes may contribute to OA via the release of factors with autocrine and paracrine tissue remodeling activity. We focused the analysis on ccl, cxcl cytokines/chemokines and ILs, for which expression was upregulated with chondrocyte hypertrophy (Table S2). Seven cytokines/chemokines were overexpressed by hypertrophic chondrocytes, especially in relation to prehypertrophic chondrocytes. Among them, only CXCL12 and IL-34 have their receptors (CXCR4, PTPRZ1 and CSF1R) also upregulated, suggesting that they may act in an autocrine loop (Table S2). Interestingly, Ptrpz1 was the most overexpressed gene during the hypertrophic differentiation of chondrocytes (72.1-fold increased expression compared to iMACs), just after Mmp3. In contrast, the levels of Cxcr7, the second receptor of CXCL12, were unchanged.

Since the involvement of IL-34 in OA is unknown, we next focused our investigation on its expression in OA. Consistent with the microarray analysis, RT-qPCR confirmed the overexpression of Il-34, Ptprz1 and Csf1r in hypertrophic chondrocytes (n=6) (Fig. 4A-C). Both Il-34 and Ptprz1 mRNA levels increased progressively during the hypertrophic differentiation of chondrocytes, whereas the increase in the expression of Csf1r mRNA was observed during the conversion of iMACs to prehypertrophic chondrocytes. Concentrations of IL-34 in both cell supernatants and cell lysates also increased with iMAC hypertrophic differentiation (Fig. 4D and E). Similar results were also observed during the hypertrophic differentiation of human chondrocytes. Their hypertrophic differentiation was associated with a decrease in the mRNA levels Sox9 and aggrecan, an increase in those of TNAP and MMP-13, and the presence of areas of calcification within the extracellular matrix (Fig. S3). Human hypertrophic chondrocytes also showed an increase in IL-34 mRNA expression (Padj=0.011, 95%CI [0.22;1.17], n=7) and in IL-34

concentration in cell supernatant (Padj=0.0013, 95%CI [0.89;2.08], n=6) and cell lysates (Padj=0.0282, 95%CI [0.27;3.17], n=6) (Fig. 4F-H).

IL-34 was also released by human OA cartilage, regardless of whether it originated from articular cartilage or from the thin cartilage layer covering osteophytes (Fig. 5A). However, cartilage from osteophytes released higher amounts of IL-34 than OA articular cartilage (P=0.0368, 95%CI [23.43;506.40]). OA tissues also expressed PTPRZ1 and CSF1R (Fig. 5B). Within articular cartilage, positive immunostaining for PTPRZ1 and CSF1R was mainly detected in the chondrocytes of the deeper area of the cartilage or in clusters of chondrocytes, although not all isolated chondrocyte or chondrocyte clusters were positive (Fig. 5B, panels a-f). A more intense immunostaining was observed within the bone and was associated with osteoblasts, osteocytes and cells present in vascular channels, including vessels and mesenchymal stromal cells. A similar positive immunostaining pattern was observed within osteophytes (Fig. 5B, panels g-l). Chondrocytes, osteoblasts, osteocytes and bone marrow cells were positive for both CSF1R and PTPRZ1. In addition, mesenchymal cells of the fibrous tissue, which often covered the osteophyte surface, were also positive for PTPRZ1 immunostaining (Fig. 5B, panels j and k).

IL-34 increases the remodeling potential of hypertrophic chondrocytes and osteoblasts

We next determined the chondrocyte (n=7) and osteoblast response (n=5) to IL-34. No effect of IL-34 on iMACs and prehypertrophic chondrocytes was observed (data not shown). In contrast, both hypertrophic chondrocytes and osteoblasts were sensitive to IL-34 stimulation. A dose-dependent increase in the mRNA expression of Ccl2, Cxcl12 and

Mmp13 by hypertrophic chondrocytes was observed in response to IL-34 (Fig. 6A-C). This was associated with a dose-dependent increase in the release of CCL2 and MMP-13 (P=0.0360 and P=0.0489 for CCL2 and MMP-13, respectively) (Fig. 6E-F). No increase in MMP-3 expression and release was observed (Fig. 6D and G). Similarly, IL-34 tended to stimulate the expression of Ccl2 (P=0.0911), Mmp3 (P=0.129), Mmp13 (P=0.141) and Tnfα (P=0.1301), by osteoblasts (Fig. 7A-D). Consistently, IL-34 stimulated the release of CCL2 (P=0.0005), MMP-3 (P=0.0085) and MMP-13 (P=0.0052) by IL-34 in a dose-dependent manner (Fig. 7G-I). IL-34 induced also a dose-dependent decrease in the mRNA expression of both Pedf (P=0.0084) and Ptprz1 (P=0.0917) by osteoblasts (Fig. 7E-F). IL-34 had no observable effect on the mRNA expression of Vegf, Rankl and Csf1r in both hypertrophic chondrocytes and osteoblasts (data not shown).

Discussion

OA is characterized at the cellular level by deep phenotypic modifications of cells from the different joint tissues. Notably, there is a hypertrophic differentiation of chondrocytes leading to the accumulation of calcified depots within cartilage [19] and an advancement of the mineralization front in the deeper part of the cartilage. Hypertrophic differentiation of chondrocytes during OA is thought to play an important role in cartilage disappearance and subchondral bone remodeling [20, 21]. Therefore, the identification of molecular factors produced by hypertrophic chondrocytes and involved in cartilage and bone damage in OA could be of therapeutic interest. However, no current model of chondrocyte hypertrophic differentiation is able to lead such investigations. None use articular chondrocytes to obtain hypertrophic chondrocytes able to calcify their matrix. Either they do not provide sufficient quantities of hypertrophic chondrocytes or are based on cell lines rather than primary cultures.

Thus, developing such a model that combines all these features represents a real need and a great challenge. Here, we have developed an original model of progressive articular chondrocyte hypertrophic differentiation and identified the recently discovered IL-34 as a factor with putative osteochondral remodeling activity.

Our model of chondrocyte hypertrophic differentiation was achieved starting with primary cultures of iMACs. Calcification was only observed after culturing iMACs successively in Medium 1, Medium 2 and then in Medium 3. In addition, only a faint expression of osteocalcin, Osterix and Tnap was observed in the iMAC cultures, suggesting that matrix calcification was not due to contamination of cultures by osteoblasts. Although a transdifferentiation of some chondrocytes into osteoblast-like cells during the culture time cannot be totally ruled out, we consider that the features we

observed are attributable to hypertrophic chondrocytes rather than osteoblast-like cells since the expression of Col10a1, a specific marker of hypertrophic chondrocytes, was strongly increased during the culture time.

Chondrocyte hypertrophy is generally only determined by the combination of an increased expression of some hypertrophic markers with the decreased expression of chondrocyte markers [22-25]. Nevertheless, in addition to these criteria, matrix calcification appears necessary to ascertain that chondrocytes reach hypertrophy. Indeed, chondrocytes cultured in Medium 2 never calcified, although they showed a mRNA expression of hypertrophic markers. The current published culture models of hypertrophic differentiation reaching matrix calcification include primary cultures of chondrocytes isolated from limb buds and growth plate, ATDC5 cells and mesenchymal stem cells (MSCs) [26-30]. However, neither ATDC5 cells nor MSCs are chondrocytes, and despite the similarities between chondrocytes from growth plates and articular cartilage, they have distinct molecular phenotypes [31-33]. These models are therefore not suitable for studying hypertrophic articular chondrocytes. Yahara *et al.* also reported matrix calcification with cultures of articular chondrocytes [17]. Pellet cultures of human OA articular chondrocytes expressed hypertrophic markers and showed calcifications [17] (and this study). However, only sparse calcifications were observed, suggesting that only a subset of chondrocytes reach hypertrophy. Nevertheless, this model appears useful to validate our results obtained with iMACs.

In addition to iMACs and hypertrophic chondrocytes, our model provides insight into a third chondrocyte phenotype, which we considered as prehypertrophic chondrocytes considering its gene expression pattern. This chondrocyte population expressed intermediate levels of chondrocyte and hypertrophic markers compared to those expressed in iMACs and hypertrophic chondrocytes, and they did not calcify their matrix. These cells

also expressed known prehypertrophic markers, including snorc and osteomodulin [9, 34], whose expression was stronger than that in both iMACs and hypertrophic chondrocytes. The prehypertrophic phenotype corresponded to a specific population of chondrocytes showing a homogeneous molecular pattern, as revealed by PCA of the microarray results. The whole genome transcriptomic analysis indeed revealed that two phenotypically distinct populations of chondrocytes were obtained from iMACs. We characterized them as prehypertrophic and hypertrophic chondrocytes based on their gene expression pattern and their ability to calcify or not their extracellular matrix. Investigating other features, including the cell shape and the composition and the organization of the extracellular matrix, would be of interest to validate prehypertrophic and hypertrophic states.

The presence of several populations of cells with molecularly distinct phenotypes within articular cartilage has recently been described in human OA cartilage [35, 36]. Ji *et al.* characterized seven different chondrocyte populations, including prehypertrophic and hypertrophic chondrocytes [36]. Their results suggest that prehypertrophic chondrocytes localized in the deeper part of articular cartilage play an important role in OA progression. Here, we show that prehypertrophic chondrocytes is the most sensitive chondrocyte population to an inflammatory stimulus. Inflammatory stress is a hallmark of OA, and IL-1β induced a more potent global response by prehypertrophic chondrocytes than by iMACs and hypertrophic chondrocytes. In addition, the prehypertrophic to hypertrophic differentiation of chondrocytes is associated with an increase in the bone remodeling and angiogenic potential of chondrocytes, as evaluated by their molecular pattern. Functional studies will be needed to ascertain the increased potential for tissue remodeling of hypertrophic chondrocytes.

The microarray analysis for cytokines/chemokines overexpressed with chondrocyte hypertrophic differentiation and able to act in an autocrine and paracrine manner

highlighted the recently discovered IL-34 [37]. RT-qPCR results confirmed this increased mRNA expression, and we also showed that murine and human chondrocytes produced IL-34 at higher rates when chondrocytes were hypertrophic. In OA, hypertrophic chondrocytes are localized within articular cartilage and osteophytes, where they are suspected to play a major role in the pathological remodeling of the osteochondral junctions. Both articular and osteophytic cartilages from OA patients released IL-34. A differential transcriptomic analysis of articular and osteophytic cartilage from paired OA patients revealed a higher expression of genes with functions in terminal chondrocyte differentiation by osteophytic cartilage [38]. Interestingly, we found that osteophytic cartilage released higher amounts of IL-34 than articular cartilage. In addition, PTRZ1 was among the most upregulated genes in osteophytic cartilage compared to its gene expression in articular cartilage [38]. Both osteophytic and articular cartilages showed positive immunostaining of PTPRZ1. In particular, OA cartilage PTPRZ1-positive chondrocytes were preferentially located in the deeper zone of joint cartilage or in the chondrocyte clusters, the two areas where hypertrophic chondrocytes are usually found [7, 19]. Osteoblasts and osteocytes of the subchondral bone also express PTPRZ1, as described [39], as well as cells present in vascular channels, including vessels and mesenchymal stromal cells. We found a similar expression pattern for CSF1R, whose the expression by bone cells and the increased expression in OA cartilage has been already reported by others [40, 41].

Considering the expression of IL-34 and its receptors by cells of the cartilage/subchondral bone interface, IL-34 may act as a paracrine and autocrine factor on cartilage and bone cells in OA. IL-34 is indeed a known osteoclastogenesis factor [42, 43] and has been reported to stimulate angiogenesis [44]. Its biological activity on both chondrocytes and osteoblasts has never been investigated. Neither iMACs nor prehypertrophic chondrocytes responded to IL-34 stimulation. This may be explained by the differential

expression of IL-34 receptors on iMACs, prehypertrophic and hypertrophic chondrocytes. However, the involvement of other molecular partners differentially produced by the phenotypically distinct chondrocytes cannot be excluded as IL-34 displays some of its biological activities independently to Ptprz1 and Csf1r. It may also bind to other cytokines to form heteromeric cytokines [45, 46]. In hypertrophic chondrocytes and osteoblasts, IL-34 stimulated the mRNA expression and the release of some tissue remodeling factors, especially the mRNA expression of Cxcl12 in hypertrophic chondrocytes, the secretion of CCL2 and MMP-13 by hypertrophic chondrocytes and osteoblasts and the release of MMP-3 by osteoblasts. Although IL-34 did not stimulate VEGF expression, it may indirectly induce angiogenesis by stimulating the expression of CXCL12 and by inhibiting that of the angiostatic factor PEDF. In addition to its reported direct action on osteoclastogenesis and angiogenesis [42-44], IL-34 may thus indirectly stimulate these two processes by acting on hypertrophic chondrocytes and osteoblasts. Cartilage-derived IL-34 may also explain the positive association between IL-34 concentration in synovial fluid and the radiographic and symptomatic severity of knee OA [47]. Further studies are needed to explore the specific role of IL-34, especially on human hypertrophic chondrocytes and osteoblasts, and more precisely that of hypertrophic-derived IL-34 in OA.

Some limitations emerge from our study. They include the characterization of our model of iMAC hypertrophic differentiation, which would be enriched with the study of the cell shape and the extracellular matrix composition and organization. Functional studies are also needed to ascertain the increased potential for tissue remodeling of hypertrophic chondrocytes and the role of IL-34.

To conclude, we have developed a new model of articular chondrocyte hypertrophic differentiation, which allows obtaining three molecularly distinct populations: iMACs, prehypertrophic chondrocytes and matrix calcifying hypertrophic chondrocytes. Our

results support the hypothesis that the phenotypic alterations of prehypertrophic chondrocytes in articular cartilage are critical for the loss of cartilage homeostasis observed in OA. The prehypertrophic to hypertrophic differentiation of chondrocytes induced the expression of a subset of genes, which together may favor the pathological remodeling of cartilage and bone, as observed in OA. Notably, the increased production of IL-34 by hypertrophic chondrocytes could act locally on hypertrophic chondrocytes and osteoblasts to indirectly stimulate osteoclastogenesis and angiogenesis. Therefore, according to the tissue remodeling potential of the recently discovered IL-34, further investigations are needed to determine whether IL-34 could be targeted in OA and/or may be used as a synovial biomarker to determine the severity of OA.

Acknowledgments

This work was supported by grants from the Société Française de Rhumatologie and the Fondation Arthritis Courtin. We thank Sébastien Mallinger for his technical assistance. Sandy van Eegher was supported by a PhD grant from the Ministère de l'Enseignement Supérieur et de la Recherche. Indira Toillon was supported by a PhD grant from the region Ile de France (ARDoC program). Stéphanie Malbos was supported by a grant from the Société Française de Rhumatologie.

Author Contributions

- Conception and design: MHLP, PP, GRV, FDC, FB, XH
- Analysis and interpretation of the data: SVE, MLPL, IT, DV, CB, SCG, LG, MHLP, PP, GRV, FDC, FB, XH
- Drafting of the article: SVE, DV, FB, XH
- Critical revision of the article for important intellectual content: DV, FB, XH
- Final approval of the article: SVE, MLPL, IT, DV, AP, DC, CB, SCG, LG, DC, SM, GN, AS, MHLP, PP, GRV, FDC, FB, XH
- Provision of study materials or patients: AS
- Statistical expertise: DV
- Obtaining of funding: FP, MHLP, FDC, FB, XH
- Collection and assembly of data: SVE, MLPL, IT, AP, DC, CB, DC, SM, GN, AS, XH

Role of the funding source

This work was supported by grants from the Société Française de Rhumatologie and the Fondation Arthritis Courtin. Sandy van Eegher was supported by a PhD grant from the Ministère de l'Enseignement Supérieur et de la Recherche. Indira Toillon was supported by a PhD grant from the region Ile de France (ARDoC program). Stéphanie Malbos was supported by a grant from the Société Française de Rhumatologie.

Competing interests

None.

References

1. Troeberg L,Nagase H. Proteases involved in cartilage matrix degradation in osteoarthritis. Biochim Biophys Acta 2011;1824(1):133-45.
2. Goldring SR,Goldring MB. Changes in the osteochondral unit during osteoarthritis: structure, function and cartilage-bone crosstalk. Nat Rev Rheumatol 2016;12(11):632-44.
3. Lories RJ,Luyten FP. The bone-cartilage unit in osteoarthritis. Nat Rev Rheumatol 2011;7(1):43-9.
4. Mahjoub M, Berenbaum F,Houard X. Why subchondral bone in osteoarthritis? The importance of the cartilage bone interface in osteoarthritis. Osteoporos Int 2012;23 Suppl 8(841-6.
5. Zuscik MJ, Hilton MJ, Zhang X, Chen D,O'Keefe RJ. Regulation of chondrogenesis and chondrocyte differentiation by stress. J Clin Invest 2008;118(2):429-38.
6. Aigner T, Bertling W, Stoss H, Weseloh G,von der Mark K. Independent expression of fibril-forming collagens I, II, and III in chondrocytes of human osteoarthritic cartilage. J Clin Invest 1993;91(3):829-37.
7. Pullig O, Weseloh G, Ronneberger D, Kakonen S,Swoboda B. Chondrocyte differentiation in human osteoarthritis: expression of osteocalcin in normal and osteoarthritic cartilage and bone. Calcif Tissue Int 2000;67(3):230-40.
8. Wachsmuth L, Soder S, Fan Z, Finger F,Aigner T. Immunolocalization of matrix proteins in different human cartilage subtypes. Histol Histopathol 2006;21(5):477-85.
9. Belluoccio D, Etich J, Rosenbaum S, Frie C, Grskovic I, Stermann J, *et al.* Sorting of growth plate chondrocytes allows the isolation and characterization of cells of a defined differentiation status. J Bone Miner Res 2010;25(6):1267-81.

10. Muller C, Khabut A, Dudhia J, Reinholt FP, Aspberg A, Heinegard D, *et al.* Quantitative proteomics at different depths in human articular cartilage reveals unique patterns of protein distribution. Matrix Biol 2014;40(34-45.
11. Semevolos SA, Nixon AJ, Fortier LA, Strassheim ML,Haupt J. Age-related expression of molecular regulators of hypertrophy and maturation in articular cartilage. J Orthop Res 2006;24(8):1773-81.
12. Vortkamp A, Lee K, Lanske B, Segre GV, Kronenberg HM,Tabin CJ. Regulation of rate of cartilage differentiation by Indian hedgehog and PTH-related protein. Science 1996;273(5275):613-22.
13. Priam S, Bougault C, Houard X, Gosset M, Salvat C, Berenbaum F, *et al.* Identification of soluble 14-3-3 as a novel subchondral bone mediator involved in cartilage degradation in osteoarthritis. Arthritis Rheum 2013;65(7):1831-42.
14. Sanchez C, Gabay O, Salvat C, Henrotin YE,Berenbaum F. Mechanical loading highly increases IL-6 production and decreases OPG expression by osteoblasts. Osteoarthritis Cartilage 2009;17(4):473-81.
15. Gosset M, Berenbaum F, Thirion S,Jacques C. Primary culture and phenotyping of murine chondrocytes. Nat Protoc 2008;3(8):1253-60.
16. Salvat C, Pigenet A, Humbert L, Berenbaum F,Thirion S. Immature murine articular chondrocytes in primary culture: a new tool for investigating cartilage. Osteoarthritis Cartilage 2005;13(3):243-9.
17. Yahara Y, Takemori H, Okada M, Kosai A, Yamashita A, Kobayashi T, *et al.* Pterosin B prevents chondrocyte hypertrophy and osteoarthritis in mice by inhibiting Sik3. Nat Commun 2016;7(10959.

18. Hughes TR, Mao M, Jones AR, Burchard J, Marton MJ, Shannon KW, *et al.* Expression profiling using microarrays fabricated by an ink-jet oligonucleotide synthesizer. Nat Biotechnol 2001;19(4):342-7.
19. Kirsch T, Swoboda B,Nah H. Activation of annexin II and V expression, terminal differentiation, mineralization and apoptosis in human osteoarthritic cartilage. Osteoarthritis Cartilage 2000;8(4):294-302.
20. Dreier R. Hypertrophic differentiation of chondrocytes in osteoarthritis: the developmental aspect of degenerative joint disorders. Arthritis Res Ther 2010;12(5):216.
21. Singh P, Marcu KB, Goldring MB,Otero M. Phenotypic instability of chondrocytes in osteoarthritis: on a path to hypertrophy. Ann N Y Acad Sci 2018;
22. Cecil DL, Johnson K, Rediske J, Lotz M, Schmidt AM,Terkeltaub R. Inflammation-induced chondrocyte hypertrophy is driven by receptor for advanced glycation end products. J Immunol 2005;175(12):8296-302.
23. Pesesse L, Sanchez C, Delcour JP, Bellahcene A, Baudouin C, Msika P, *et al.* Consequences of chondrocyte hypertrophy on osteoarthritic cartilage: potential effect on angiogenesis. Osteoarthritis Cartilage 2013;21(12):1913-23.
24. Wehling N, Palmer GD, Pilapil C, Liu F, Wells JW, Muller PE, *et al.* Interleukin-1beta and tumor necrosis factor alpha inhibit chondrogenesis by human mesenchymal stem cells through NF-kappaB-dependent pathways. Arthritis Rheum 2009;60(3):801-12.
25. Zhang X, Crawford R,Xiao Y. Inhibition of vascular endothelial growth factor with shRNA in chondrocytes ameliorates osteoarthritis. J Mol Med (Berl) 2016;94(7):787-98.

26. James CG, Ulici V, Tuckermann J, Underhill TM,Beier F. Expression profiling of Dexamethasone-treated primary chondrocytes identifies targets of glucocorticoid signalling in endochondral bone development. BMC Genomics 2007;8(205.
27. Stanton LA, Sabari S, Sampaio AV, Underhill TM,Beier F. p38 MAP kinase signalling is required for hypertrophic chondrocyte differentiation. Biochem J 2004;378(Pt 1):53-62.
28. Kirsch T, Nah HD, Shapiro IM,Pacifici M. Regulated production of mineralization-competent matrix vesicles in hypertrophic chondrocytes. J Cell Biol 1997;137(5):1149-60.
29. Mueller MB,Tuan RS. Functional characterization of hypertrophy in chondrogenesis of human mesenchymal stem cells. Arthritis Rheum 2008;58(5):1377-88.
30. Shukunami C, Ishizeki K, Atsumi T, Ohta Y, Suzuki F,Hiraki Y. Cellular hypertrophy and calcification of embryonal carcinoma-derived chondrogenic cell line ATDC5 in vitro. J Bone Miner Res 1997;12(8):1174-88.
31. Chau M, Lui JC, Landman EB, Spath SS, Vortkamp A, Baron J, *et al.* Gene expression profiling reveals similarities between the spatial architectures of postnatal articular and growth plate cartilage. PLoS One 2014;9(7):e103061.
32. Hissnauer TN, Baranowsky A, Pestka JM, Streichert T, Wiegandt K, Goepfert C, *et al.* Identification of molecular markers for articular cartilage. Osteoarthritis Cartilage 2010;18(12):1630-8.
33. Matsusaki T, Aoyama T, Nishijo K, Okamoto T, Nakayama T, Nakamura T, *et al.* Expression of the cadherin-11 gene is a discriminative factor between articular and growth plate chondrocytes. Osteoarthritis Cartilage 2006;14(4):353-66.
34. Heinonen J, Taipaleenmaki H, Roering P, Takatalo M, Harkness L, Sandholm J, *et al.* Snorc is a novel cartilage specific small membrane proteoglycan expressed in

differentiating and articular chondrocytes. Osteoarthritis Cartilage 2011;19(8):1026-35.

35. Jayasuriya CT, Hu N, Li J, Lemme N, Terek R, Ehrlich MG, *et al.* Molecular characterization of mesenchymal stem cells in human osteoarthritis cartilage reveals contribution to the OA phenotype. Sci Rep 2018;8(1):7044.

36. Ji Q, Zheng Y, Zhang G, Hu Y, Fan X, Hou Y, *et al.* Single-cell RNA-seq analysis reveals the progression of human osteoarthritis. Ann Rheum Dis 2018;78(1):100-10.

37. Lin H, Lee E, Hestir K, Leo C, Huang M, Bosch E, *et al.* Discovery of a cytokine and its receptor by functional screening of the extracellular proteome. Science 2008;320(5877):807-11.

38. Gelse K, Ekici AB, Cipa F, Swoboda B, Carl HD, Olk A, *et al.* Molecular differentiation between osteophytic and articular cartilage--clues for a transient and permanent chondrocyte phenotype. Osteoarthritis Cartilage 2012;20(2):162-71.

39. Kaspiris A, Mikelis C, Heroult M, Khaldi L, Grivas TB, Kouvaras I, *et al.* Expression of the growth factor pleiotrophin and its receptor protein tyrosine phosphatase beta/zeta in the serum, cartilage and subchondral bone of patients with osteoarthritis. Joint Bone Spine 2013;80(4):407-13.

40. Wittrant Y, Gorin Y, Mohan S, Wagner B,Abboud-Werner SL. Colony-stimulating factor-1 (CSF-1) directly inhibits receptor activator of nuclear factor-{kappa}B ligand (RANKL) expression by osteoblasts. Endocrinology 2009;150(11):4977-88.

41. Rai MF, Tycksen ED, Cai L, Yu J, Wright RW,Brophy RH. Distinct degenerative phenotype of articular cartilage from knees with meniscus tear compared to knees with osteoarthritis. Osteoarthritis Cartilage 2019;27(6):945-55.

42. Baud'huin M, Renault R, Charrier C, Riet A, Moreau A, Brion R, *et al.* Interleukin-34 is expressed by giant cell tumours of bone and plays a key role in RANKL-induced osteoclastogenesis. J Pathol 2010;221(1):77-86.
43. Chen Z, Buki K, Vaaraniemi J, Gu G,Vaananen HK. The critical role of IL-34 in osteoclastogenesis. PLoS One 2011;6(4):e18689.
44. Segaliny AI, Mohamadi A, Dizier B, Lokajczyk A, Brion R, Lanel R, *et al.* Interleukin-34 promotes tumor progression and metastatic process in osteosarcoma through induction of angiogenesis and macrophage recruitment. Int J Cancer 2015;137(1):73-85.
45. Segaliny AI, Brion R, Brulin B, Maillasson M, Charrier C, Teletchea S, *et al.* IL-34 and M-CSF form a novel heteromeric cytokine and regulate the M-CSF receptor activation and localization. Cytokine 2015;76(2):170-81.
46. Segaliny AI, Brion R, Mortier E, Maillasson M, Cherel M, Jacques Y, *et al.* Syndecan-1 regulates the biological activities of interleukin-34. Biochim Biophys Acta 2015;1853(5):1010-21.
47. Wang SL, Zhang R, Hu KZ, Li MQ,Li ZC. Interleukin-34 Synovial Fluid Was Associated with Knee Osteoarthritis Severity: A Cross-Sectional Study in Knee Osteoarthritis Patients in Different Radiographic Stages. Dis Markers 2018;2018(2095480.

Figure legends

Figure 1. Hypertrophic chondrocyte differentiation markers assessed in iMACs differentiated into prehypertrophic and hypertrophic chondrocytes.

A) Model of progressive hypertrophic differentiation of iMACs. iMACs isolated from the femoral heads and the knees of newborn mice were cultured for seven days in Medium 1. Confluent iMACs were then cultured for 28 days in Medium 2 to obtain prehypertrophic chondrocytes and for an additional 42 days for prehypertrophic to hypertrophic phenotype changes. **B–N)** Gene expression pattern of articular chondrocyte markers **(B-E)**, prehypertrophic markers **(F-H)** and hypertrophic markers **(I-N)** in iMACs, prehypertrophic chondrocytes and hypertrophic chondrocytes from 6 independent cell cultures. The results are expressed as fold expression compared to those of iMACs, whose mRNA expression was set to 1 for each culture. **O)** Measurement of alkaline phosphatase activity associated with iMACs, prehypertrophic chondrocytes and hypertrophic chondrocytes (n=8). Lower panels, representative photomicrographs of the cytochemical determination of phosphatase alkaline activity in iMACs, prehypertrophic chondrocytes and hypertrophic chondrocytes. **P)** Quantification of chondrocyte culture mineralization by alizarin red staining (n=12). Lower panels, representative photomicrographs of alizarin red staining of iMACs, prehypertrophic chondrocytes and hypertrophic chondrocytes. Only hypertrophic chondrocytes showed positive alizarin red staining. Bars indicate the mean expression levels.

Figure 2. Whole-genome transcriptomic characterization across iMAC differentiation processes into hypertrophic chondrocytes.

Results from differential analysis of gene expression in the chondrocytes. Signatures of differentially expressed genes (DEG) identified between **A)** hypertrophic vs articular chondrocytes (n=8 in each group), **B)** prehypertrophic vs articular (n=8 in each group), **C)** and hypertrophic vs prehypertrophic chondrocytes (n=8 in each group). A Venn diagram compares the signatures obtained. Each comparison is illustrated by a hierarchical clustering (correlation distance on genes and Euclidean distance on samples). Volcano plots present the log2-fold changes and the significance of each gene for the 3 comparisons. Gene and probe numbers differ due to repeated spotting and/or missing annotations.

Figure 3. Loss of the prehypertrophic phenotype shifts chondrocytes towards an OA-inducing phenotype.

A-G) iMACs, prehypertrophic chondrocytes and hypertrophic chondrocytes from 6 independent cell cultures were stimulated by IL-1β (1 ng/mL) for 24 hours, and the mRNA expression of Col2a1 **(A)**, Acan **(B)**, Il-6 **(C)**, Mmp13 **(D)**, Vegf **(E)**, Tsp1 **(F)** and Chm1 **(G)** was determined. **H-K)** Phenotypic transition of prehypertrophic to hypertrophic chondrocytes induces the expression of factors involved in OA. Prehypertrophic and hypertrophic chondrocytes from 6 to 12 independent cell cultures were assessed for the mRNA expression of matrix proteases **(H)**, osteoblast **(I)** and osteoclast activity **(J)** and angiogenic/angiostatic factors **(K)**. Data are expressed as fold expression compared to those in unstimulated control cells, whose mRNA expression was set to 1 for each culture

(A-G), or to that in prehypertrophic chondrocytes **(H-K)**. Bars indicate the mean expression levels.

Figure 4. Increased expression of IL-34 and IL-34 receptors with chondrocyte hypertrophic differentiation.

A-E) mRNA expression of Il-34 **(A)**, Ptprz1 **(B)** and Csf1r **(C)** in iMACs, prehypertrophic chondrocytes and hypertrophic chondrocytes (n = 6) was determined. **C-D)** IL-34 protein levels were quantified by ELISA in cell conditioned medium (n = 7) **(D)** and cell lysates (n = 6) **(E)** of iMACs, prehypertrophic chondrocytes and hypertrophic chondrocytes. **F-H)** The IL-34 mRNA expression (n = 7) **(F)** and protein levels (n = 6) in chondrocyte conditioned medium **(G)** and cell lysates **(H)** were determined in human control and hypertrophic chondrocytes.

Figure 5. Expression of IL-34 and IL-34 receptors in OA.

A) IL-34 secreted by articular (n = 14 different donors) and osteophyte cartilages (n = 6 different donors) from OA patients was measured in tissue conditioned media by ELISA. **B)** Paraffin sections (5 µm) of OA cartilage bone interface (a-f) and osteophytes (g-l) (n = 5 to 8 different donors) were stained for CSF1R (a, b, g and h), PTPRZ1 (d, e, j and k) or with irrelevant antibodies as negative controls (c, f, i and l). CSF1- and PTPRZ1-positive staining are observed at the osteochondral junction (a, b, d and e). Chondrocytes near the tidemark express both the IL-34 receptors CSF1R and PTPRZ1. Within the bone, CSF1R- and PTPRZ1-positive staining is associated with osteoblasts and vascular channels. Similar staining was observed for both CSF1R and PTPRZ1 within osteophytes (g, h, j and k). Chondrocytes, osteoblasts, osteocytes and bone marrow cells showed positive staining. In

addition, mesenchymal cells of the fibrous tissue at the osteophyte surface were positive for PTPRZ1. Panels b, e, h and k show higher magnification views of the delimited areas of panels a, d, g and j, respectively. Cartilage and bone are delimited by dotted lines. Bo: bone, Cart: cartilage, CC: calcified cartilage. Bars = 200 µm (a, d, g and j) or 50 µm (b, c, e, f, h, i, k and l).

Figure 6. Increased remodeling potential of hypertrophic chondrocytes in response to IL-34.

Hypertrophic chondrocytes (n=7) were stimulated by increasing concentrations of IL-34 before RT-qPCR analysis of the mRNA expression of Cxcl12 **(A)**, Ccl2 **(B)**, Mmp3 **(C)** and Mmp13 **(D)**. The release of CCL2 **(E)**, MMP-3 **(F)** and MMP-13 **(G)** into cell conditioned medium in response to increased concentrations of IL-34 was measured by ELISAs.

Figure 7. Increased remodeling potential of osteoblasts in response to IL-34.

Osteoblasts (n=5) were stimulated by increasing concentrations of IL-34 before RT-qPCR analysis of the mRNA expression of Cxcl12 Ccl2 **(A)**, Mmp3 **(B)**, Mmp13 **(C),** Tnfα **(D)**, Pedf **(E)** and Ptprz1 **(F)**. The release of CCL2 **(G)**, MMP-3 **(H)** and MMP-13 **(J)** into cell conditioned medium in response to increased concentrations of IL-34 was measured by ELISAs.

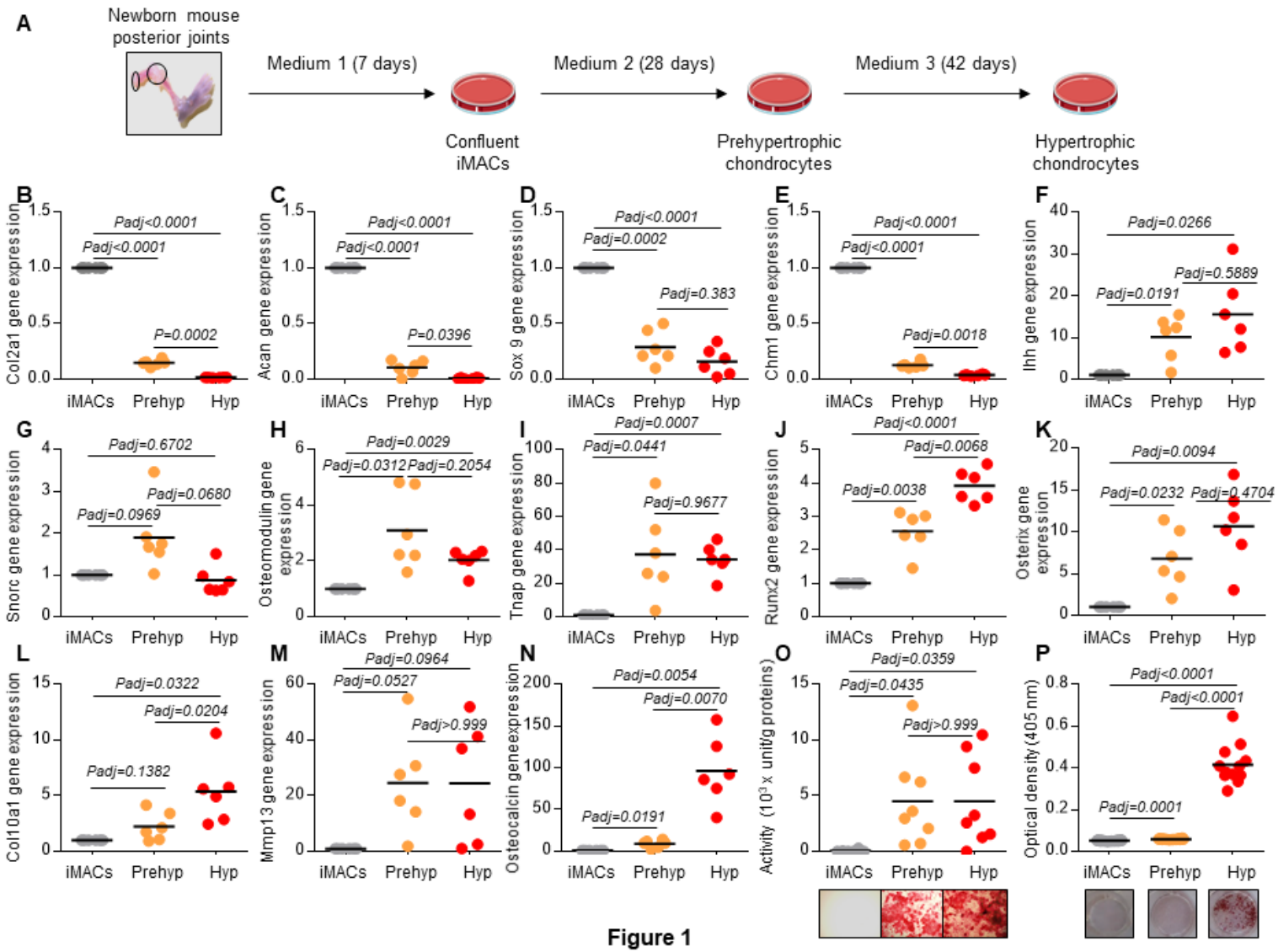
A
Newborn mouse posterior joints
Medium 1 (7 days)
Medium 2 (28 days)
Medium 3 (42 days)
Confluent iMACs
Prehypertrophic chondrocytes
Hypertrophic chondrocytes
B
Col2a1 gene expression
Padj<0.0001
Padj<0.0001
P=0.0002
C
Acan gene expression
Padj<0.0001
Padj<0.0001
P=0.0396
D
Sox 9 gene expression
Padj<0.0001
Padj=0.0002
Padj=0.383
E
Chm1 gene expression
Padj<0.0001
Padj<0.0001
Padj=0.0018
F
Ihh gene expression
Padj=0.0266
Padj=0.0191
Padj=0.5889
G
Snorc gene expression
Padj=0.6702
Padj=0.0680
Padj=0.0969
H
Osteomodulin gene expression
Padj=0.0029
Padj=0.0312
Padj=0.2054
I
Tnap gene expression
Padj=0.0007
Padj=0.0441
Padj=0.9677
J
Runx2 gene expression
Padj<0.0001
Padj=0.0068
Padj=0.0038
K
Osterix gene expression
Padj=0.0094
Padj=0.0232
Padj=0.4704
L
Col10a1 gene expression
Padj=0.0322
Padj=0.0204
Padj=0.1382
M
Mmp13 gene expression
Padj=0.0964
Padj=0.0527
Padj>0.999
N
Osteocalcin geneexpression
Padj=0.0054
Padj=0.0070
Padj=0.0191
O
Activity (10³ x unit/g proteins)
Padj=0.0359
Padj=0.0435
Padj>0.999
P
Optical density (405 nm)
Padj<0.0001
Padj<0.0001
Padj=0.0001
iMACs
Prehyp
Hyp

Figure 1

705

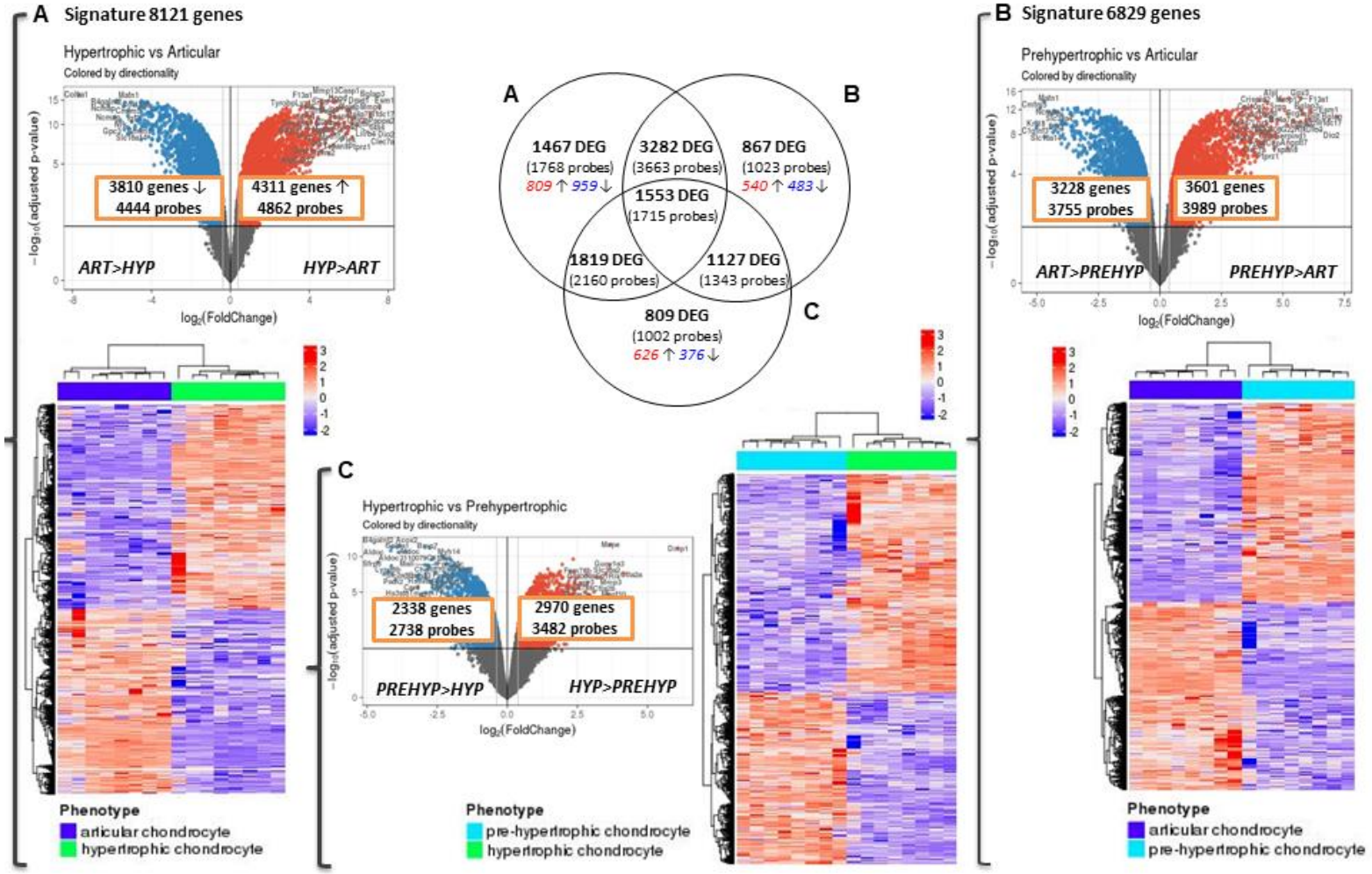
A Signature 8121 genes
Hypertrophic vs Articular
Colored by directionality
3810 genes ↓
4444 probes
4311 genes ↑
4862 probes
ART>HYP
HYP>ART
log2(FoldChange)
Phenotype
articular chondrocyte
hypertrophic chondrocyte
A
B
C
1467 DEG
(1768 probes)
809 ↑ 959 ↓
3282 DEG
(3663 probes)
867 DEG
(1023 probes)
540 ↑ 483 ↓
1553 DEG
(1715 probes)
1819 DEG
(2160 probes)
1127 DEG
(1343 probes)
809 DEG
(1002 probes)
626 ↑ 376 ↓
C
Hypertrophic vs Prehypertrophic
Colored by directionality
2338 genes
2738 probes
2970 genes
3482 probes
PREHYP>HYP
HYP>PREHYP
log2(FoldChange)
Phenotype
pre-hypertrophic chondrocyte
hypertrophic chondrocyte
B Signature 6829 genes
Prehypertrophic vs Articular
Colored by directionality
3228 genes
3755 probes
3601 genes
3989 probes
ART>PREHYP
PREHYP>ART
log2(FoldChange)
Phenotype
articular chondrocyte
pre-hypertrophic chondrocyte

Figure 2

706

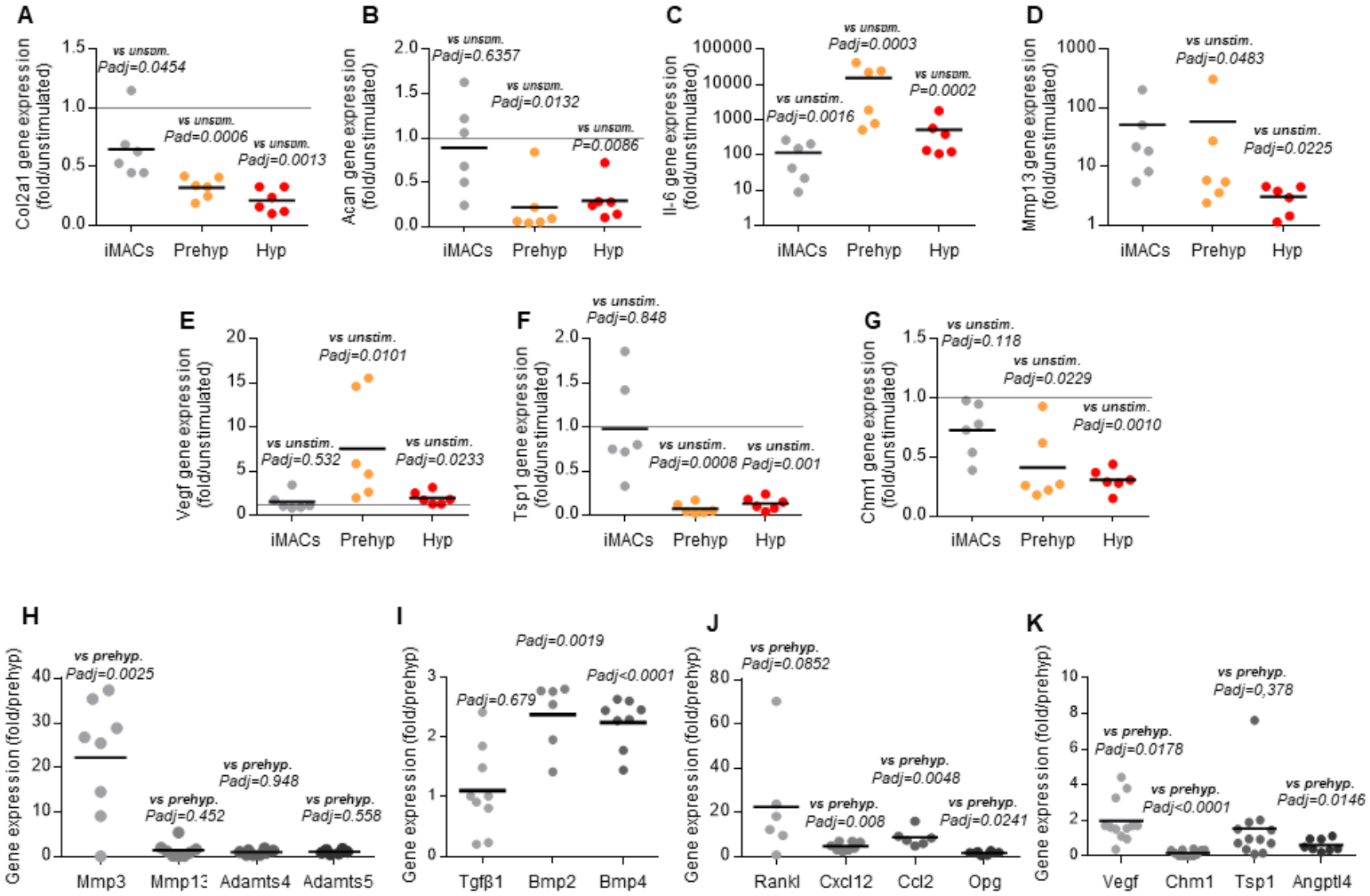
A
Col2a1 gene expression (fold/unstimulated)
vs unstim. Padj=0.0454
vs unstim. Pad=0.0006
vs unstim. Padj=0.0013
iMACs Prehyp Hyp
B
Acan gene expression (fold/unstimulated)
vs unstim. Padj=0.6357
vs unstim. Padj=0.0132
vs unstim. P=0.0086
iMACs Prehyp Hyp
C
Il-6 gene expression (fold/unstimulated)
vs unstim. Padj=0.0003
vs unstim. Padj=0.0016
vs unstim. P=0.0002
iMACs Prehyp Hyp
D
Mmp13 gene expression (fold/unstimulated)
vs unstim. Padj=0.0483
vs unstim. Padj=0.0225
iMACs Prehyp Hyp
E
Vegf gene expression (fold/unstimulated)
vs unstim. Padj=0.0101
vs unstim. Padj=0.532
vs unstim. Padj=0.0233
iMACs Prehyp Hyp
F
Tsp1 gene expression (fold/unstimulated)
vs unstim. Padj=0.848
vs unstim. Padj=0.0008
vs unstim. Padj=0.001
iMACs Prehyp Hyp
G
Chm1 gene expression (fold/unstimulated)
vs unstim. Padj=0.118
vs unstim. Padj=0.0229
vs unstim. Padj=0.0010
iMACs Prehyp Hyp
H
Gene expression (fold/prehyp)
vs prehyp. Padj=0.0025
vs prehyp. Padj=0.452
vs prehyp. Padj=0.948
vs prehyp. Padj=0.558
Mmp3 Mmp13 Adamts4 Adamts5
I
Gene expression (fold/prehyp)
Padj=0.0019
Padj=0.679
Padj<0.0001
Tgfβ1 Bmp2 Bmp4
J
Gene expression (fold/prehyp)
vs prehyp. Padj=0.0852
vs prehyp. Padj=0.008
vs prehyp. Padj=0.0048
vs prehyp. Padj=0.0241
Rankl Cxcl12 Ccl2 Opg
K
Gene expression (fold/prehyp)
vs prehyp. Padj=0,378
vs prehyp. Padj=0.0178
vs prehyp. Padj<0.0001
vs prehyp. Padj=0.0146
Vegf Chm1 Tsp1 Angptl4

Figure 3

707

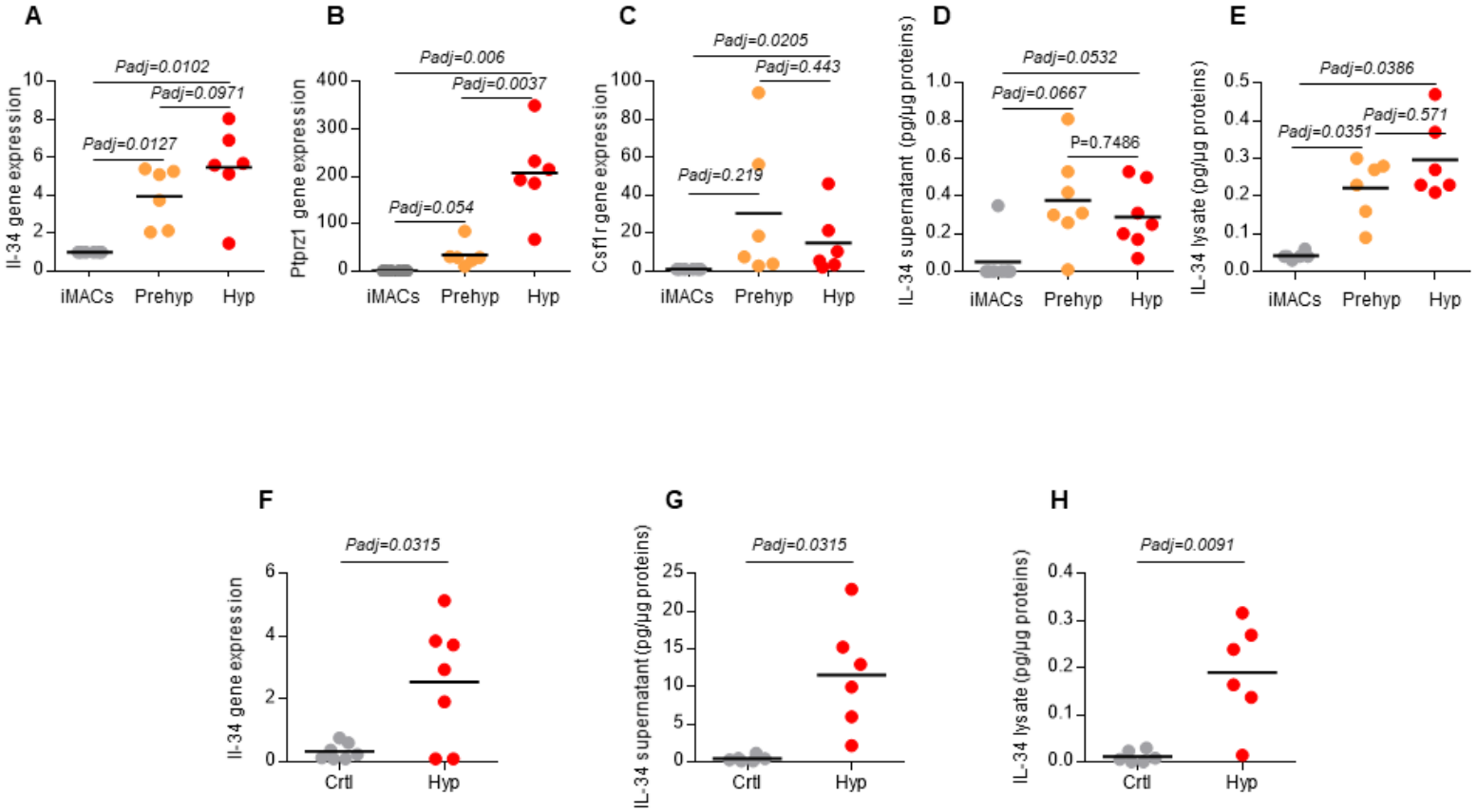
A
Il-34 gene expression
Padj=0.0102
Padj=0.0971
Padj=0.0127
iMACs
Prehyp
Hyp
B
Ptprz1 gene expression
Padj=0.006
Padj=0.0037
Padj=0.054
C
Csf1r gene expression
Padj=0.0205
Padj=0.443
Padj=0.219
D
IL-34 supernatant (pg/µg proteins)
Padj=0.0532
Padj=0.0667
P=0.7486
E
IL-34 lysate (pg/µg proteins)
Padj=0.0386
Padj=0.571
Padj=0.0351
F
Il-34 gene expression
Padj=0.0315
Crtl
Hyp
G
IL-34 supernatant (pg/µg proteins)
Padj=0.0315
H
IL-34 lysate (pg/µg proteins)
Padj=0.0091

Figure 4

708

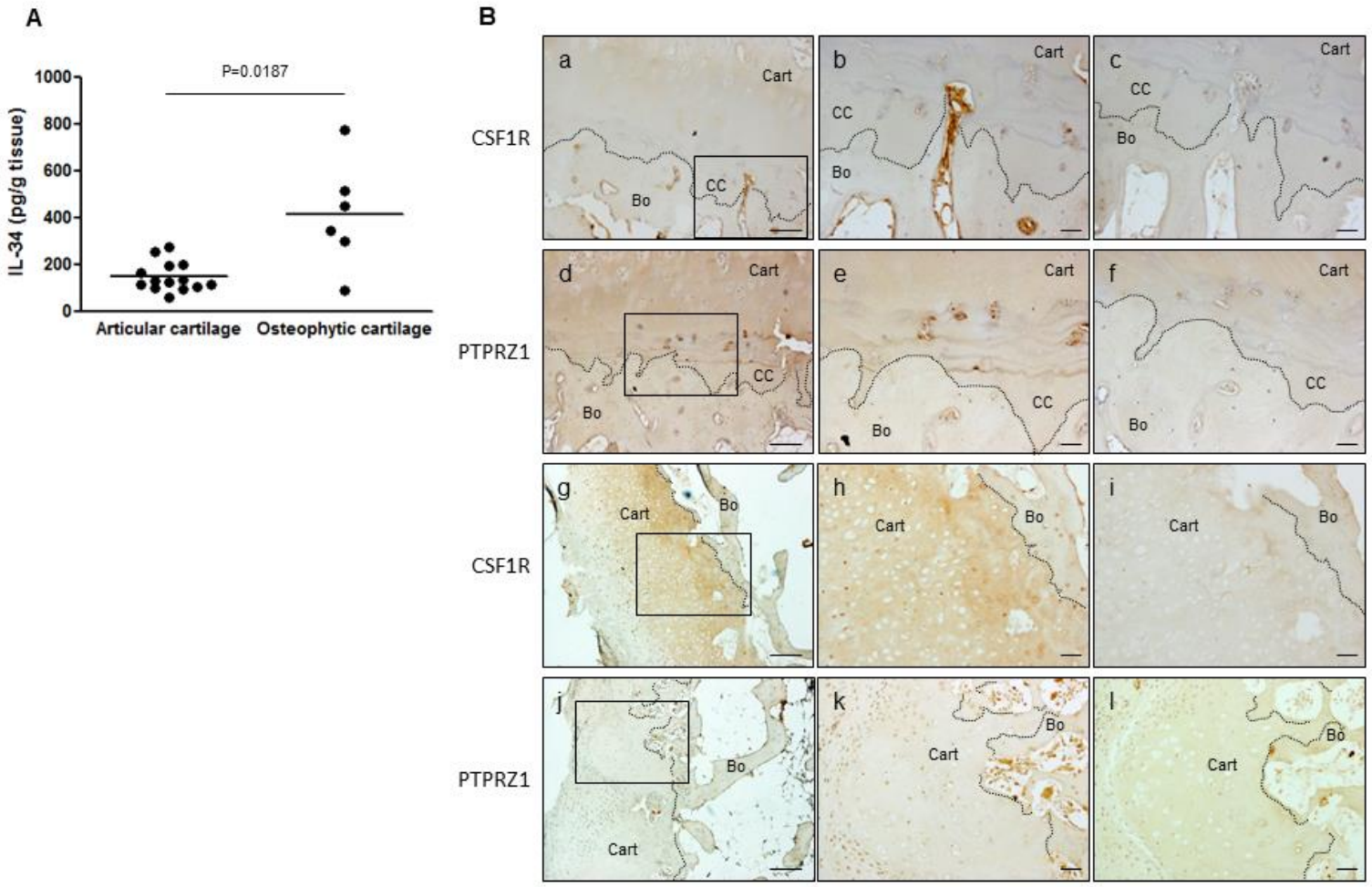
A
P=0.0187
IL-34 (pg/g tissue)
1000
800
600
400
200
0
Articular cartilage
Osteophytic cartilage
B
CSF1R
PTPRZ1
CSF1R
PTPRZ1
a
b
c
d
e
f
g
h
i
j
k
l
Cart
Bo
CC

Figure 5

709

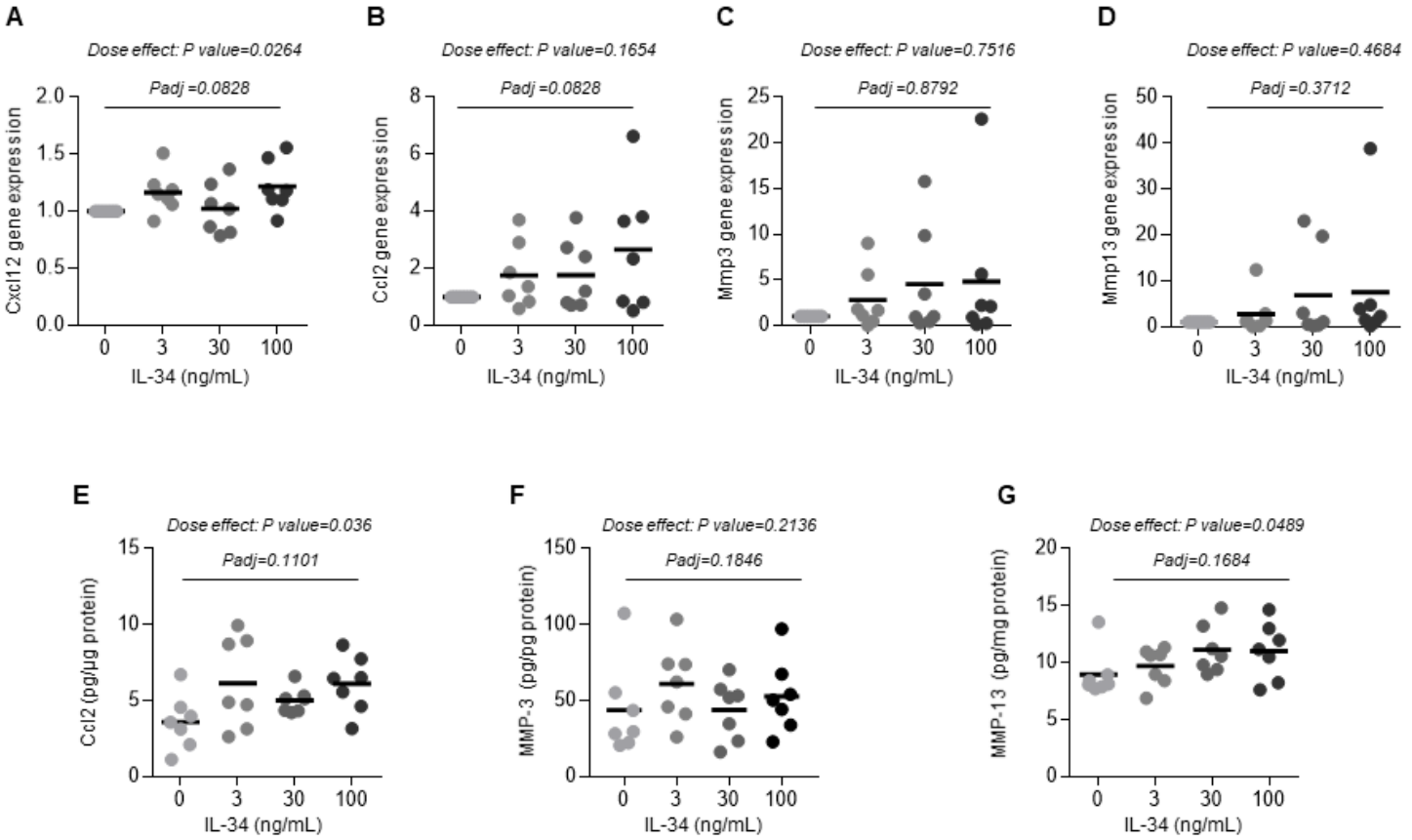
A
Dose effect: P value=0.0264
Padj =0.0828
Cxcl12 gene expression
IL-34 (ng/mL)
B
Dose effect: P value=0.1654
Padj =0.0828
Ccl2 gene expression
IL-34 (ng/mL)
C
Dose effect: P value=0.7516
Padj =0.8792
Mmp3 gene expression
IL-34 (ng/mL)
D
Dose effect: P value=0.4684
Padj =0.3712
Mmp13 gene expression
IL-34 (ng/mL)
E
Dose effect: P value=0.036
Padj=0.1101
Ccl2 (pg/µg protein)
IL-34 (ng/mL)
F
Dose effect: P value=0.2136
Padj=0.1846
MMP-3 (pg/pg protein)
IL-34 (ng/mL)
G
Dose effect: P value=0.0489
Padj=0.1684
MMP-13 (pg/mg protein)
IL-34 (ng/mL)

Figure 6

710

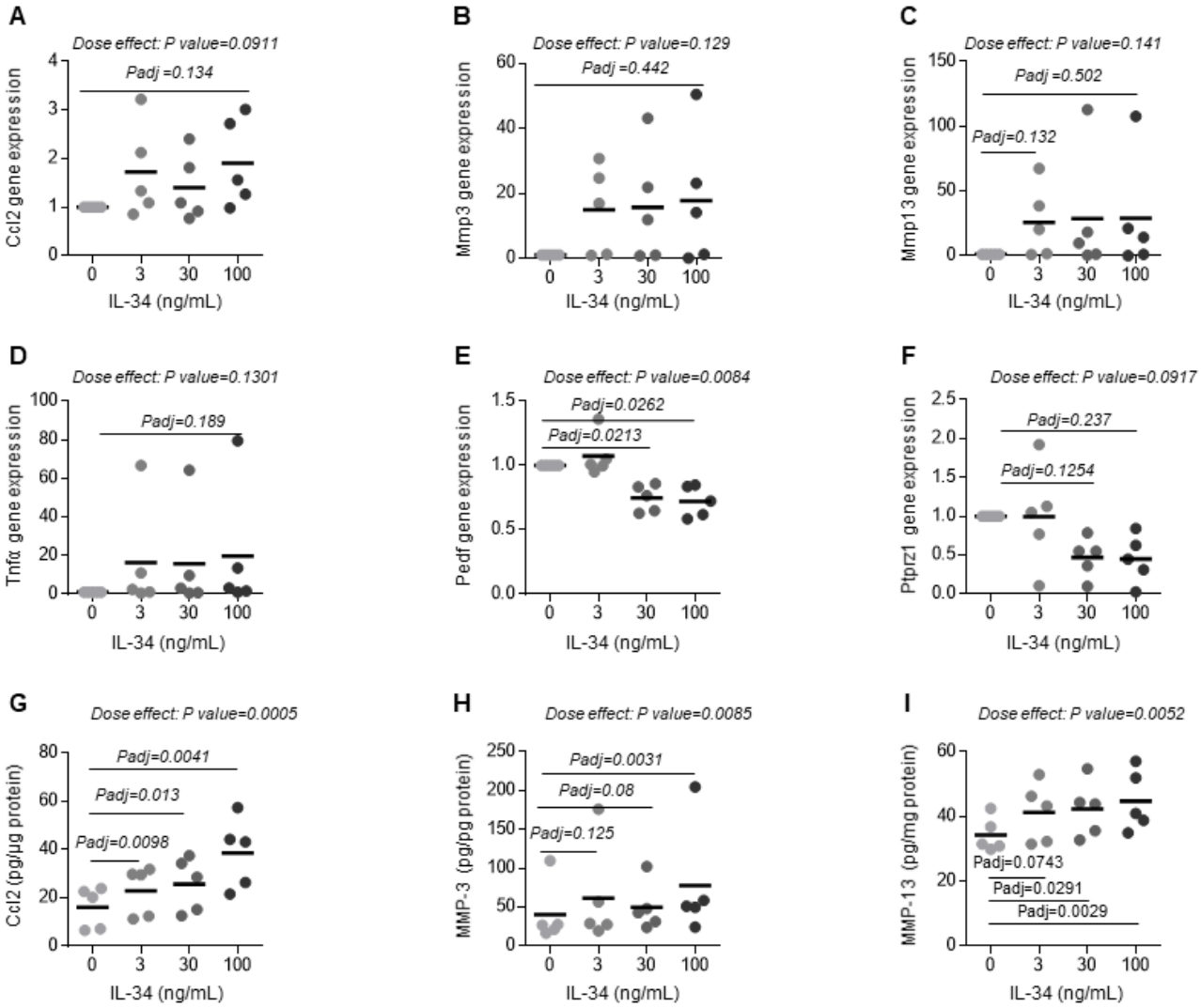
A
Dose effect: P value=0.0911
Padj =0.134
Ccl2 gene expression
IL-34 (ng/mL)
B
Dose effect: P value=0.129
Padj =0.442
Mmp3 gene expression
IL-34 (ng/mL)
C
Dose effect: P value=0.141
Padj =0.502
Padj=0.132
Mmp13 gene expression
IL-34 (ng/mL)
D
Dose effect: P value=0.1301
Padj=0.189
Tnfα gene expression
IL-34 (ng/mL)
E
Dose effect: P value=0.0084
Padj=0.0262
Padj=0.0213
Pedf gene expression
IL-34 (ng/mL)
F
Dose effect: P value=0.0917
Padj=0.237
Padj=0.1254
Ptprz1 gene expression
IL-34 (ng/mL)
G
Dose effect: P value=0.0005
Padj=0.0041
Padj=0.013
Padj=0.0098
Ccl2 (pg/µg protein)
IL-34 (ng/mL)
H
Dose effect: P value=0.0085
Padj=0.0031
Padj=0.08
Padj=0.125
MMP-3 (pg/pg protein)
IL-34 (ng/mL)
I
Dose effect: P value=0.0052
Padj=0.0743
Padj=0.0291
Padj=0.0029
MMP-13 (pg/mg protein)
IL-34 (ng/mL)

Figure 7

711

Supplementary Information

Materials and methods

Collection of osteoarthritis human cartilage and subchondral bone

Human OA knee explants were obtained from 33 patients undergoing total knee joint replacement surgery for OA in the Department of Orthopedic Surgery and Traumatology of Saint-Antoine Hospital and in the Maussins-Nollet Clinic (Paris, France). Informed consent was obtained from each patient on the day before the arthroplasty. Experiments using human samples have been approved by two French Institutional Review Boards (Comité de Protection des Personnes Ile de France V; Comité Consultatif sur le Traitement de l'information en Matière de Recherche). The mean age of patients was 69.6±11.2 years and 78.8% were women. The mean BMI was 30.1±4.5 kg/m^2.

Tissue pieces from the middle part of the medial and lateral tibial plateaus and femoral condyles were preserved for histological analysis. The remaining cartilage from each joint compartment was separated from the underlining bone and cut into small pieces (1 mm^3) before a 24-hour incubation at 37°C in RPMI culture medium supplemented with 100 U/mL penicillin, 100 µg/mL streptomycin and 4 mM glutamine, as described [1]. Conditioned media was then separated from tissues and centrifuged at 3000 g for 5 min to remove the debris. Conditioned media and tissues were stored at -80°C for further analysis. Alternatively, chondrocytes were isolated for cell culture experiments.

Immunohistochemistry

Tissue samples were fixed in 3.7% paraformaldehyde for 2 days and decalcified in a solution of 14% ethylenediaminetetraacetic acid in distilled water (pH 7.4) for 4 to 6 weeks at 4°C. Samples were embedded in paraffin wax and serially sectioned (5 µm).

Immunohistochemistry was performed with a mouse monoclonal antibody against PTPRZ1 (clone 12/RPTPb, BD Transduction Laboratories; dilution 1:50) and a rabbit polyclonal antibody against CSF-1R (H-300, Santa Cruz Biotechnology; dilution 1:50) as the primary antibodies. Enzyme-induced antigen retrieval was performed as follows: 0.2 mg/mL hyaluronidase in phosphate-buffered saline (PBS) (pH 5.5) for 10 min at 37°C and then 0.1 mg/mL pronase in PBS (pH 7.4) for 20 min at 37°C for CD34, OC and PTP-ζ, and 2 mg/mL hyaluronidase in PBS (pH 5.5) for 10 min at 37°C and 1 mg/mL pronase in PBS (pH 7.4) for 20 min at 37°C for CSF-1R. The R.T.U. Vectastain kit (Vector) was used for detection, followed by counterstaining with Mayer's hematoxylin. Irrelevant control antibodies (Dako) were incubated at the same concentration to assess nonspecific staining. Preparations were mounted in Eukitt medium. Digital images of magnification views (10X) of whole-tissue sections were captured by using an Olympus SC50 camera on an Olympus IX83 microscope.

Primary culture of murine articular chondrocytes and differentiation into hypertrophic chondrocytes

Immature articular chondrocytes (iMACs) were isolated from the femoral heads and knees of 5-6-day-old newborn C57BL/6 mice (Janvier labs) and cultured in DMEM culture medium (1 g/L glucose) supplemented with fetal calf serum (10%), penicillin (100 U/mL), streptomycin (100 µg/mL) and L-glutamine (4 mM)) (Medium 1) for 7 days, as described [2, 3]. For each independent cell culture, iMACs were pooled from 5 to 7 newborn littermates. After the cells were seeded in the culture plates, the culture wells containing the cells were randomly allocated to the different experimental groups. Prehypertrophic chondrocytes were obtained by culturing chondrocytes for an additional 28 days in culture medium 2 consisting of DMEM/HAM-F12 medium supplemented with fetal calf serum

762 (5%), penicillin (100 U/mL), streptomycin (100 µg/mL) and L-glutamine (4 mM), ascorbic
763 acid (40 µg/mL, Sigma-Aldrich), insulin-transferrin-sodium selenite (1%, Sigma-Aldrich)
764 and triiodo-L-thyronine (50 ng/mL, Sigma-Aldrich) (Medium 2). Prehypertrophic
765 chondrocytes were further cultured for 42 days in the latter medium supplemented with β-
766 glycerophosphate (10 mM, Sigma-Aldrich), retinoic acid (100 nM, Sigma-Aldrich) and
767 1α,25-dihydroxyvitamin D_3 (10 nM, Sigma-Aldrich) (Medium 3) to obtain hypertrophic
768 chondrocytes. All cultures were performed at 37°C in a humidified atmosphere of 5%
769 CO_2/95% air with the exception of the prehypertrophic to hypertrophic differentiation step,
770 which was performed at 37°C in a humidified atmosphere of 3% CO_2/95% air. At the end
771 of the culture, chondrocytes were washed 2 times with PBS and incubated in DMEM (1
772 g/L glucose) without serum for 4 hours. Chondrocytes were then washed with PBS and
773 further incubated in DMEM without serum for 24 hours. Conditioned media were then
774 kept, centrifuged and stored at -20°C. Cells were either fixed in 3.7% paraformaldehyde
775 (PFA) for cytological analysis or used for mRNA or protein extraction.
776

777 **Primary culture of murine osteoblasts**

778 Osteoblasts were isolated from the calvaria of 5- to 6-day-old newborn C57BL/6 mice
779 (Janvier labs), as previously described [4]. For each independent cell culture, osteoblasts
780 were pooled from 5 to 7 newborn littermates. After the cells were seeded in the culture
781 plates, the culture wells containing the cells were randomly allocated to the different
782 experimental groups. Briefly, osteoblasts were cultured for 21 days in DMEM/HAM-F12
783 supplemented with fetal calf serum (10%), penicillin (100 U/mL), streptomycin (100
784 µg/mL), L-glutamine (4 mM), and ascorbic acid (50 µg/mL, Sigma-Aldrich). After 10 days
785 of culture, β-glycerophosphate (5 mM, Sigma-Aldrich) was added to the culture medium.
786 At the end of the culture, osteoblasts were washed 2 times with PBS and incubated in

DMEM (1 g/L glucose) without serum for 4 hours. Osteoblasts were then washed with PBS and further incubated in DMEM without serum for 24 hours. Conditioned media were then kept, centrifuged and stored at -20°C. Cells are used for mRNA extraction.

All experiments with murine chondrocytes and osteoblasts were performed according to the protocols approved by French and European ethics committees (Comité d'Ethique en Expérimentation Animale n°5 Charles Darwin de la Région Ile de France).

Stimulation of primary cultures of murine chondrocytes and osteoblasts

Before treatment, iMACs, prehypertrophic chondrocytes, hypertrophic chondrocytes or osteoblasts were cultured for 24 hours in serum-free DMEM (1 g/L glucose) containing penicillin (100 U/mL) and streptomycin (100 µg/mL). Cells were stimulated in the same medium by human recombinant IL-1β (1 ng/mL) (PeproTech) or murine recombinant IL-34 (PeproTech) at increasing concentrations (3, 30 and 100 ng/mL). After 24 hours of stimulation, the supernatants and total RNA were kept and stored at -80°C.

Primary culture of human articular chondrocytes and differentiation into hypertrophic chondrocytes

Human chondrocytes were isolated from the less damaged areas of OA cartilage from patients who underwent total knee arthroplasty. The hypertrophic differentiation of human articular chondrocytes was performed according to Yahara *et al.* [5]. A total of 10^6 chondrocytes were seeded into 10-cm dishes and cultured for 7 days in chondrogenic medium, which was composed of DMEM (4.5 g/L glucose), fetal calf serum (10%), L-glutamine (4 mM), penicillin (100 U/mL), streptomycin (100 µg/mL), insulin-transferrin-sodium selenite solution (1%, Sigma-Aldrich), recombinant human transforming growth

factor-beta 1 (TGF-β_1) (10 ng/mL, PeproTech), dexamethasone (100 nM, Sigma-Aldrich), sodium pyruvate (1 mM, Sigma-Aldrich) and L(+)-ascorbic acid (50 µg/mL, Sigma-Aldrich). Then, 5.10^5 cells were transferred into 15-mL polypropylene tubes, pelleted by centrifugation for 10 min at 500 g and cultured in the same medium for 3 days. Pellets were transferred into 24-well culture plates and cultured for 8 weeks in the same medium. The medium was replaced with DMEM (4.5 g/L glucose), 1% fetal calf serum, L-glutamine (4 mM), penicillin (100 U/mL), streptomycin (100 µg/mL), 1% insulin-transferrin-sodium selenite (Sigma-Aldrich), recombinant human bone morphogenetic protein-2 (BMP-2) (10 ng/mL, PeproTech), recombinant human growth differentiation factor-5 (GDF-5) (10 ng/mL, PeproTech), triiodo-L-thyronine (1 µM, Sigma Aldrich), dexamethasone (10 nM, Sigma-Aldrich), L(+)-ascorbic acid (50 µg/mL, Sigma-Aldrich) and β-glycerophosphate (10 mM, Sigma-Aldrich) for 2 additional weeks. At the end of the culture, chondrocytes were washed 2 times with PBS and incubated in DMEM (1 g/L glucose) without serum for 4 hours. Pellets were then washed with PBS and further incubated in DMEM without serum for 24 hours. Conditioned media were then kept, centrifuged and stored at -20°C. Cell pellets were lysed for mRNA or protein extraction. Some pellets were fixed in 3.7% PFA and embedded in paraffin. The presence of calcification was revealed by von Kossa staining on microsections (5 µm).

RNA extraction, reverse transcription and quantitative real-time PCR

Total RNA was extracted with the RNeasy Mini Kit (Qiagen, Courtaboeuf, France), according to the manufacturer's instructions, and the concentrations were determined using a spectrophotometer (Eppendorf, Le Pecq, France). The RNA integrity was assessed based on the 28S/18S ribosomal RNA ratio using the RNA 6000 Nano Lab-On-Chip with an Agilent 2100 Bioanalyzer (Agilent Technologies, Palo Alto, CA). All RNA samples

included in this study had an RIN >8.3. RNA (500 ng) and were reverse transcribed (RT) using an Omniscript RT Kit (Qiagen, Courtaboeuf, France). The mRNA expression of genes of interest was analyzed by quantitative real-time PCR using the Light Cycler 480 (Roche Diagnostics, Meylan, France) in a 12 µL final volume reaction using specific primers (10 µM) (see Supplementary Tables 3 and 4) and GoTaq® qPCR Master Mix (Promega Corp., Madison, WI, USA). The PCR amplification conditions were as follows: initial denaturation for 5 min at 95°C followed by 40 cycles consisting of 10 s at 95°C, 15 s at 60°C and 10 s at 72°C. For each PCR experiment, the cDNAs were run in duplicate in parallel with serial dilutions of a cDNA mixture tested for each primer pair to generate a standard linear curve, which was used to estimate the amplification efficiency. The relative mRNA expression for all genes analyzed was normalized to that of hypoxanthine guanine phosphoribosyl transferase (Hprt) or RNA ribosomal 18S (18S), used as internal reference genes for mouse and human genes, respectively, and the expression was determined using the $2^{-\Delta\Delta Ct}$ method. For the selection of samples before microarray analysis, normalization of qPCR data was realized according the gold standard proposed by Vandersompele *et al.*, 2002 [6]implemented in GeNorm software that further evolved and was integrated in qBase Plus software. We assessed the expression of 7 housekeeping genes: *Tbp, Hmbs, Actb, Ppia, Gusb, RPS18, GAPDH, RPL30* that were confirmed to be robust reference genes in our laboratory in multiple experiments. Thus, we compute M-values to identify the genes that covary the most between samples that are the most likely to enter in the computation of a normalizator. Normalizator is the geometric mean of most covarying genes that is substracted to the value of Ct of the sample. Thus, we obtain -dCt (compared to mean of invariant selected housekeeping genes using qBase+) and Fold Changes [2^-ΔΔ Ct] (each -dCt sample is compared to -dCt mean of iMACs).

Microarray analysis

To select a sufficient design for microarray analysis, we evaluated among 12 independent cultures the most representative cultures of each differentiation group, according to the gene expression of markers of each chondrocyte phenotype, and set up a method for this purpose. Eight cultures were determined to be optimal to ensure sufficient power to avoid unnecessary mouse sacrifices. Score-based selection determined that 7 cultures needed to be selected for microarray analyses (Fig. S2A). Combining the method with the best PCA contributions to the principal component 1 (PC1) group allowed us to finally select the 8 cultures among the 12 needed for the microarray experiments that were subsequently performed.

mRNA expression profiling was performed on 8 samples per group using SurePrint G3 Mouse Gene Expression v2 8x60K Microarray (G4852B, Agilent Technologies) and SurePrint Mouse miRNA Microarray Kit v21 8x60K (G4859C, Agilent Technologies) at the Servier Research Institute (Croissy-Sur-Seine, France). Labeling reactions and hybridizations were randomized according to the chondrocyte differentiation status. For mRNA profiling, probe labeling and 60 mer-oligonucleotide microarray hybridization were performed according to the manufacturer's instructions [7]. Starting with 100 ng of purified total RNA, cDNA synthesis and *in vitro* transcription were carried out using an Agilent LowInput QuickAmp Labeling Kit (Agilent Technologies, Palo Alto, CA) in the presence of Cyanine3- and Cyanine5-CTP. The fluorescently amplified cRNAs were purified with an RNeasy column (Qiagen, France) and assessed for quantification and incorporation rate using a NanoDrop Spectrophotometer (Cyanine-3-CTP at 550 nm and Cyanine-5-CTP at 650 nm). Probe length was controlled using the Agilent 2100 Bioanalyzer (Agilent Technologies, Palo Alto, CA). The two labeled cRNA probes (825 ng each), Cy5-chondrocyte subtypes and Cy3-reference sample (pool of control DMEM RNAs), were

pooled and hybridized to SurePrint G3 Mouse Gene Expression v2 8x60K Microarray (G4852B) at 65°C for 17 hours. The reference sample corresponded to a pool of the 8 control DMEM conditions, each contributing at an equal amount to this pool. Slides were washed at room temperature in Gene Expression Wash Buffer 1 (5188-5325, Agilent Technologies) for 1 min, then at 37°C in Gene Expression Wash Buffer 2 (5188-5326, Agilent Technologies) for 1 min and finally in acetonitrile for 30 s.

An Agilent scanner and Feature Extraction 11.5.1.1 software (Agilent Technologies) were used to obtain the raw microarray data for both analyses.

Protein extraction and protein assay

Murine chondrocytes were lysed in Tris HCl (10 mM) pH 7.5, $MgCl_2$ (0.5 mM) and Triton X-100 (0.1%), as described by Kirsch *et al.* [8]. Cell homogenates were centrifuged at 10000 g for 10 min at 4°C. Supernatants were kept for analysis.

Human chondrocytes in pellets were lysed in RIPA buffer containing Tris HCl (50 mM; pH 8), NaCl (150 mM), EDTA (2 mM), NP-40 (1%), sodium deoxycholate (0.5%) and sodium dodecyl sulfate (SDS) (0.1%), supplemented with protease inhibitor cocktail cOmplete™ 1X (Roche).

Protein concentrations in cell-conditioned media were determined using the Bradford assay (Bio-Rad, Hercules, CA, USA). Protein concentrations in cell lysates were determined using the Pierce™ BCA Protein Assay Kit (Thermo Fisher Scientific), according to the manufacturer's instructions.

Alkaline phosphatase activity assay

Alkaline phosphatase enzymatic activity was measured in murine chondrocyte cell lysates using the Colorimetric Alkaline Phosphatase Assay Kit, Yellow Color (FluoroProbes, Interchim, Montluçon, France).

ELISA assessment of the IL-34, MMP-3, MMP-13 and MCP-1 levels

Commercially available ELISA kits were used to determine the concentrations of mouse MMP-3 (R&D Systems), MMP-13 (Euromedex), MCP-1 (R&D Systems), IL-34 (R&D Systems), human IL-34 (R&D Systems).

Cytology

The alkaline phosphatase activity was visualized using Naphthol AS-MX phosphate (20 mg/mL, Sigma-Aldrich) and Fast Red TR (1 mg/mL, Sigma-Aldrich) in Tris-HCl buffer (36 mM; pH 8.3).

The quantification of cell calcification was performed as described [9]. After alizarin red staining, cells were scraped in 10% (v/v) acetic acid. The solution was heated at 85°C for 10 min, transferred to ice for 5 min and centrifuged at 20000 g for 15 min. Then, 250 µL of the supernatant was mixed with 100 µL of 10% (v/v) ammonium hydroxide, and the optical density was measured in triplicate at 405 nm.

Statistical analysis

We determined sample size before conducting experiments. We performed three sets of simulations using R or using StatMate (v.2.00) assuming that we will face a beta SD of 0.5, 1 or 2 and willing a power of 80%. We found the best tradeoff to us considering number of

experimental units, lowest beta estimable but also availability of samples and feasibility of experiences to ensure the less technical biases possible. Integrating all the parameters that have to be taken into account before conducting the experiments we determine that a minimum of 5-6 samples has to be assessed in a single experiment. In an optimistic scenario with low variability we would be able to assess a mean difference of ~0.5 in 80% of the cases. To face additional variability, when it was possible we added more experimental. Some qPCR analysis had even more power since 12 observations were available.

For microarrays sample size estimation the method proposed by Pawitan *et al.* [10] - OCS plus R package- was used to estimate the number of samples needed for microarrays analysis. This methodology suggested an optimal number of n=8 samples per group (paired design). For obvious reasons of cost and experience feasibility only 8 samples per group were processed in the microarrays giving the sufficient power to properly detect the expected amount of differentially expressed genes.

For further analyses, we used parametric tests after log(x) transformation: normality on markers was verified using the D'Agostino and Pearson and Shapiro-Wilk tests. For biological interpretability, we plotted the untransformed datasets on graphs.

The qPCR normalized gene expression levels of hypertrophic markers, alkaline phosphatase activity, cell calcification degrees and release of proteins in media were compared between the iMAC, prehypertrophic and hypertrophic cells using repeated measures one-way ANOVA. Heteroscedasticity was taken into account with the Geisser-Greenhouse correction. Corrections for multiple comparisons were realized using the Tukey range test when contrasting all groups in mouse chondrocytes. For the IL-1β stimulation study, we used Dunnett's post hoc test when comparing groups of interest with an additional unstimulated group. To analyze the cell response to IL-34, we also used this

model and this post hoc testing strategy to respectively determine the global dose response effect (dose p-value in the model) and adjusted p-value for comparison with the unstimulated group (0 ng/ml).

For prehypertrophic to hypertrophic chondrocyte gene expression comparison in mice as well as gene or protein comparison in OA patients, paired t-tests were used to compare observations from the two groups of interest (*e.g.*, hypertrophic vs. control or prehypertrophic conditions). For the comparison of protein levels of IL-34 in human articular cartilage vs. osteophytic cartilage, an unpaired t-test was performed with Welch correction for unequal variance. The analyses mentioned above were performed using GraphPad Prism8 (GraphPad Software Inc., San Diego, CA, USA). Values of FC, 95%CI and P-values for all experiments are available in the appendix.

For whole-genome transcriptomic analysis, litter selection was performed to ensure sufficient power with minimum mouse sacrifice. N=8 mice was determined to be the optimal number. Based on previous RT-qPCR data obtained, we calculated a score= sum of delta (|delta Ct|) between extreme phenotypes (hypertrophic and articular) for each litter to select the most variant observations. The litter was selected if they displayed a score(i)>mean(scores).

Graphical explorations on targeted genes and whole-genome data, such as two-dimensional PCA and double hierarchical clustering, were performed with the package "mixOmics" (package "mixOmics" in R [11]) under R program writer software (http://www.r-project.org/)[12] to evaluate whether clusters appear between cells and if they were associated with differentiation groups.

Raw microarray data were analyzed with Arraystudio Omicsoft version 10.0.1.112 (QIAGEN®, Cary, NC). Data were filtered (at least 6 obs>background determined with kernel density plots: 28571 probes + standard deviation in all obs.>0.38), quantile

normalized and investigated in a hierarchical clustering and a two-dimensional PCA before differential analysis was performed to visualize the similarity/dissimilarity between individuals.

Differential analysis was performed using a general linear model (GLM) that takes the pairing between samples into account for variance and estimate computations. This was followed by moderated t-tests between the differentiation groups (iMACs, prehypertrophic chondrocytes, and hypertrophic chondrocytes). Raw p-values were adjusted for multiple testing with the BH correction to control the FDR.

Differentially expressed probes (DEPs) were investigated under a 5% significance threshold (FDR < 0.05) combined with different fold change thresholds (|FC|>1, 1.3, 1.5 and 2). Graphical multivariate explorations were performed with the same methodology as previously described.

Functional analysis of signatures was performed with Ingenuity® Pathway Analysis (IPA, Qiagen Redwood City, CA, USA). Functional enrichments were identified by Fisher's exact test. The activation status of the functions/pathways was predicted using IPA by calculating a regulation Z-score and an overlap p-value, which were based on the number of known genes of interest per pathway/function, the expression changes of these target genes and their agreement with the literature findings. It was considered significantly activated (or inhibited) with an overlap p-value≤0.05 and an IPA activation Z-score≥2.0 (or ≤−2.0). The detailed descriptions of IPA analysis are available under "Upstream Regulator Analysis", "Biological Functions Analysis", and "Ingenuity Canonical Pathways Analysis" on the IPA website (http://www.ingenuity.com).

Supplementary Figure 1. Experimental design for cell culture study on murine cells.

Three sets of experiments for chondrocyte hypertrophic differentiation were designed. In the first one, 12 independent cultures were performed for microarray analysis and the characterization of the culture model. Matrix calcification was evaluated on these 12 cultures. mRNAs from 8 among the 12 cultures were used for whole genome transcriptomic analysis after evaluating the most representative litters of each differentiation group. The mRNA expression of articular prehypertrophic and hypertrophic chondrocyte markers was determined on 6 among the 12 cultures, which were chosen at random. For all the markers studied, the mRNA expression was determined on the 6 same cultures of chondrocytes. The mRNA expression of IL-34, CSF1R and PTPRZ1 in iMACs, prehypertrophic and hypertrophic chondrocytes was studied on the same 6 cultures except one due the depletion of the mRNAs for one culture. It was then replaced by mRNAs from another culture among of the 12 performed, chosen also at random. The mRNAs of the 6 same culture were also used for the determination of changes in the expression of proteases and markers of bone formation, osteoclastogenesis and angiogenesis in hypertrophic relative to prehypertrophic chondrocytes. To the results obtained with these 6 independent cultures, we added results obtained with cultures coming from the second set of experiments (6 independent cultures), in which cells were stimulated or not with IL-1β. The effect of IL-β was first studied for 3 of these 6 cultures on a panel of genes and then on a restricted panel of genes for the 3 other cultures. In the third set of experiments, 7 independent cultures were performed to evaluate the response of chondrocytes to IL-34. In parallel, the effect of IL-34 was studied on 5 independent cultures of osteoblasts.

Supplementary Figure 2. Cellular model of hypertrophic differentiation characterization using multivariate approaches.

A) Strategy to select the best litters for microarray analyses. Total variation is computed (sum for all gene expression and delta calcification values between the hypertrophic and articular groups) to select the most diverging observations between those extreme phenotypes. B) PCA using all processed microarray gene expression values revealing the genes preferentially expressed in each group. C) Double ascendant hierarchical clustering on all processed microarray gene expression values. Hypertrophy differentiation groups clustered together naturally based on whole-genome gene expression, suggesting important signatures. Distance between observations: Euclidean, distance between genes: Pearson correlation. Aggregation methods: Ward and complete. D) Predicted activation profile focused on osteoarthritis functions. Z-scores of OA-enriched functions in prehypertrophic chondrocyte signatures and hypertrophic signatures (Z-score > |2|). Functions with Z-score <-2 are predicted to be inhibited, whereas functions with Z-score>2 are predicted to be activated.

Supplementary Figure 3. Increased expression of IL-34 and IL-34 receptors with chondrocyte hypertrophic differentiation.

Human chondrocytes were isolated from the OA cartilage of 7 patients, amplified and cultured as pellets in a chondrogenic medium and then in a hypertrophic medium. **A-D)** mRNA expression of Sox 9 **(A)**, aggrecan **(B)**, Mmp13 **(C)** and Tnap **(D)** was determined in control chondrocytes cultured in the chondrogenic medium and in hypertrophic chondrocytes cultured in the chondrogenic medium followed by culture in the hypertrophic

medium. **E)** Pellets of control (panel a) and hypertrophic chondrocytes (panel b) were analyzed for matrix mineralization by von Kossa staining.

References

1. Priam S, Bougault C, Houard X, Gosset M, Salvat C, Berenbaum F, *et al.* Identification of soluble 14-3-3 as a novel subchondral bone mediator involved in cartilage degradation in osteoarthritis. Arthritis Rheum 2013;65(7):1831-42.
2. Gosset M, Berenbaum F, Thirion S,Jacques C. Primary culture and phenotyping of murine chondrocytes. Nat Protoc 2008;3(8):1253-60.
3. Salvat C, Pigenet A, Humbert L, Berenbaum F,Thirion S. Immature murine articular chondrocytes in primary culture: a new tool for investigating cartilage. Osteoarthritis Cartilage 2005;13(3):243-9.
4. Sanchez C, Gabay O, Salvat C, Henrotin YE,Berenbaum F. Mechanical loading highly increases IL-6 production and decreases OPG expression by osteoblasts. Osteoarthritis Cartilage 2009;17(4):473-81.
5. Yahara Y, Takemori H, Okada M, Kosai A, Yamashita A, Kobayashi T, *et al.* Pterosin B prevents chondrocyte hypertrophy and osteoarthritis in mice by inhibiting Sik3. Nat Commun 2016;7(10959.
6. Vandesompele J, De Preter K, Pattyn F, Poppe B, Van Roy N, De Paepe A, *et al.* Accurate normalization of real-time quantitative RT-PCR data by geometric averaging of multiple internal control genes. Genome Biol 2002;3(7):RESEARCH0034.
7. Hughes TR, Mao M, Jones AR, Burchard J, Marton MJ, Shannon KW, *et al.* Expression profiling using microarrays fabricated by an ink-jet oligonucleotide synthesizer. Nat Biotechnol 2001;19(4):342-7.

8. Kirsch T, Nah HD, Shapiro IM,Pacifici M. Regulated production of mineralization-competent matrix vesicles in hypertrophic chondrocytes. J Cell Biol 1997;137(5):1149-60.
9. Gregory CA, Gunn WG, Peister A,Prockop DJ. An Alizarin red-based assay of mineralization by adherent cells in culture: comparison with cetylpyridinium chloride extraction. Anal Biochem 2004;329(1):77-84.
10. Pawitan Y, Murthy KR, Michiels S,Ploner A. Bias in the estimation of false discovery rate in microarray studies. Bioinformatics 2005;21(20):3865-72.
11. Le Cao KA, Gonzalez I,Dejean S. integrOmics: an R package to unravel relationships between two omics datasets. Bioinformatics 2009;25(21):2855-6.
12. Team. RDC. R: a language and environment for statistical computing. . R Foundation for Statistical Computing 2011;Vienna, Austria

Experiment 1. Characterization of iMACs, prehypertrophic and hypertrophic chondrocytes *(Figures 1, 2, 3, 4 and S3)*

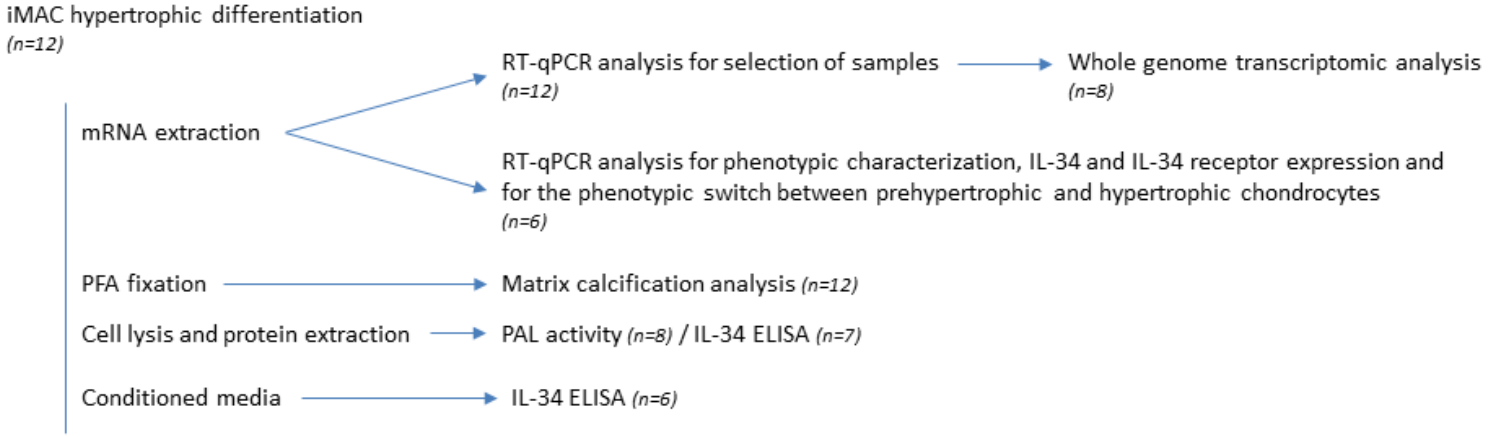

Experiment 2. Effect of IL-1β *(Figure 3)*

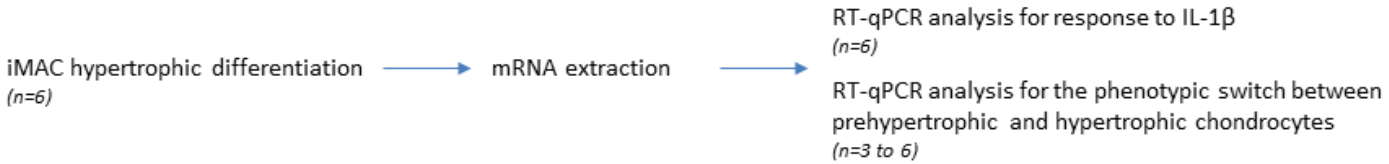

Experiment 3. Effect of IL-34 *(Figures 6 and 7)*

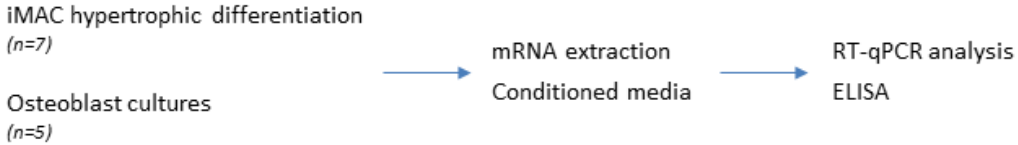

Figure S1

1092

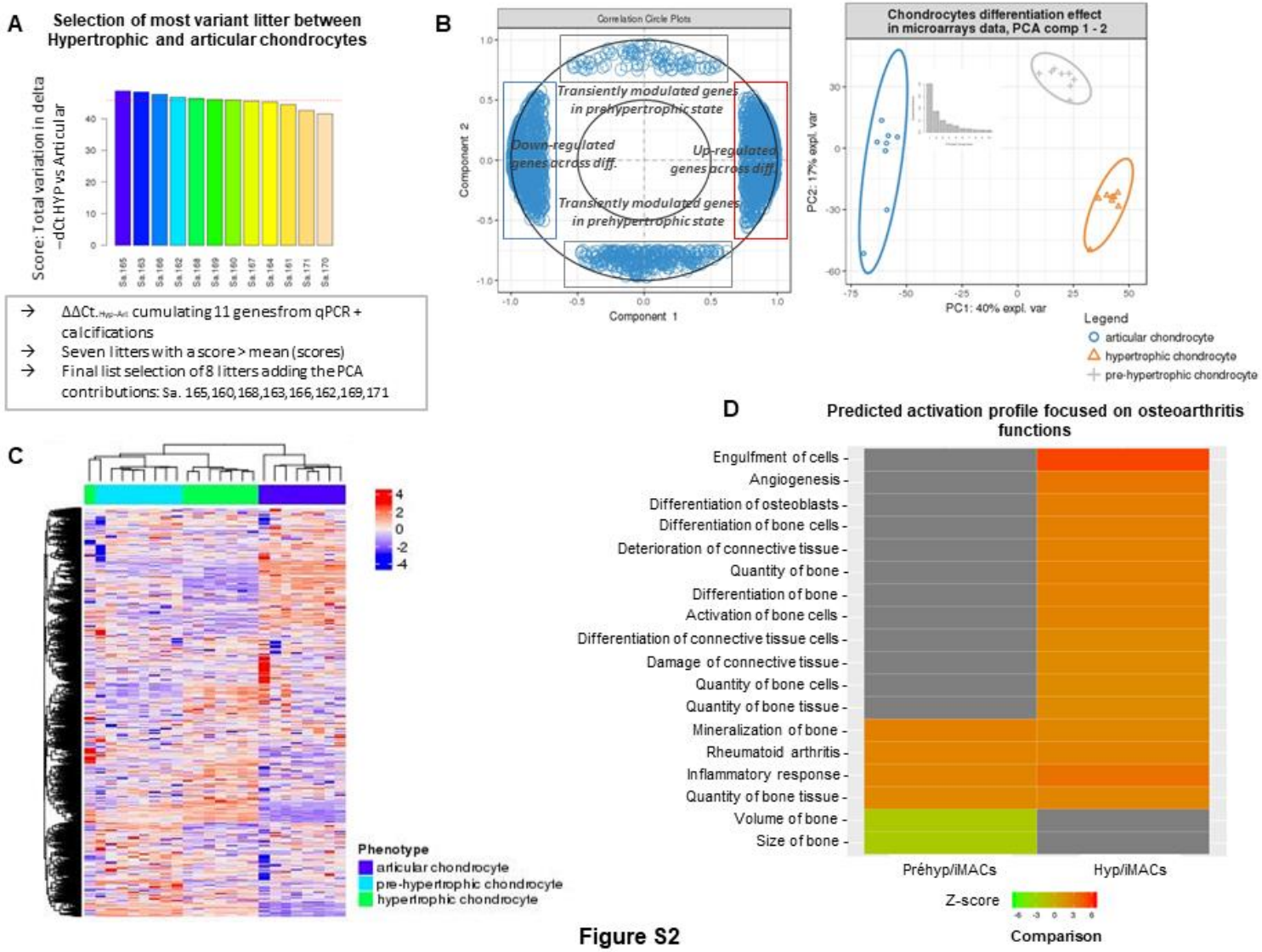

Figure S2

1093

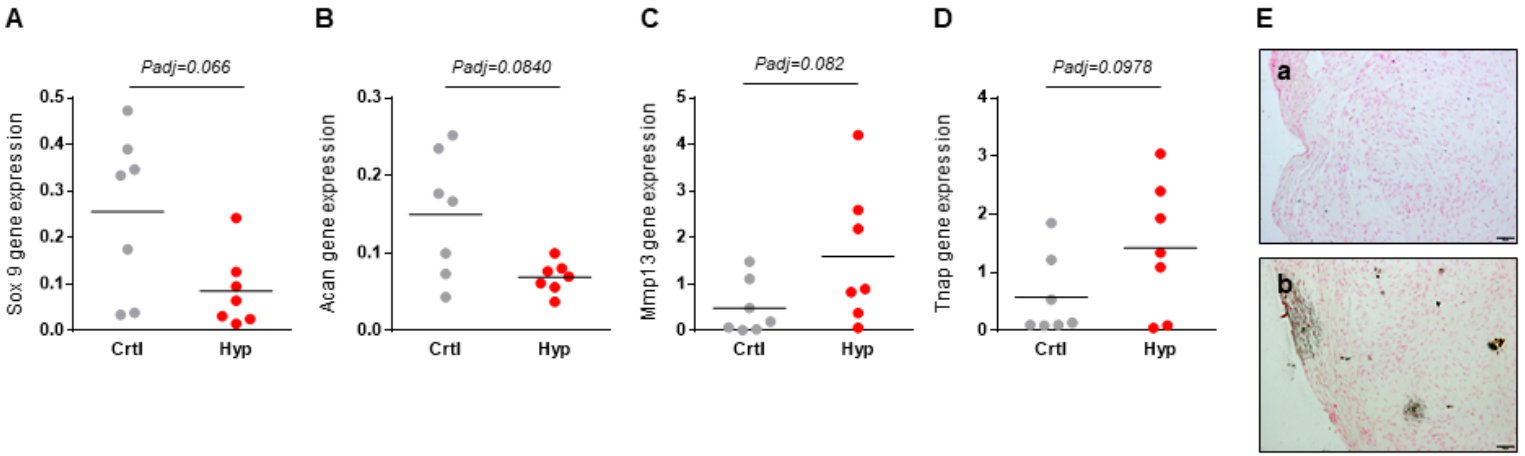

Figure S3

1094

Figure S2. A-B

Osteocalcin Staining linear regression	
Spearman r	0,371
95% confidence interval	0.02184 to 0.6404
P value (two-tailed)	0,033

Osteocalcin (ng/g tissue) linear regression	
Spearman r	0,389
95% confidence interval	0.07454 to 0.6336
P value (two-tailed)	0,014

Figure 1. A-P

RM one way ANOVA (on raw data)

Variable	Pr	
	Mean Diff. (raw values)	95.00% CI of diff.
COL2A1	-0,8519	-0.8898 to -0.8139
ACAN	-0,895	-0.9796 to -0.8104
SOX9	-0,7117	-0.9139 to -0.5094
ChM-I	-0,8727	-0.9087 to -0.8368
Ihh	9,109	2.071 to 16.15
Snorc	0,8967	-0.2019 to 1.995
Osteomodulin	2,098	0.2573 to 3.939
TNAP	36,32	1.283 to 71.35
RunX2	1,559	0.7358 to 2.382
Osterix	5,775	1.083 to 10.47
Col10a1	1,245	-0.4804 to 2.971
MMP13	23,62	-0.3613 to 47.6
Osteocalcin	7,807	1.773 to 13.84
Activity	4,452	0.15 to 8.754
Optical density	0,00725	0.004274 to 0.01023

Figure 3. A-G

RM one way ANOVA (on log transfo)

Variable	IMAC	
	Mean Diff. (log values)	95.00% CI of diff.
Col2a1	-0,2117	-0.4178 to -0.005655
Acan	-0,1274	-0.5346 to 0.2797
IL-6	1,81	1.012 to 2.608
MMP13	1,383	0.6208 to 2.145
VEGF	0,1162	-0.1992 to 0.4316
TSP1	-0,0707	-0.4228 to 0.2814
ChM-I	-0,1587	-0.3658 to 0.0484

Figure 3. H-K

Paired t tests (on raw data)

Variable	Mean of differences vs. Prehyp (raw values)	95.00% CI of diff.
MMP3	21,21	10.29 to 32.14
MMP13	0,4913	-0.9685 to 1.951
ADAMTS4	0,01375	-0.4677 to 0.4952
ADAMTS5	0,12	-0.3716 to 0.6116
TGFB1	0,1033	-0.4510 to 0.6576
BMP2	1,382	0.7836 to 1.980
BMP4	1,246	0.8958 to 1.597
RANKL	21,55	-4.319 to 47.43
CXCL12	3,801	2.192 to 5.41
CCL2	7,73	3.598 to 11.86
OPG	0,7513	0.1318 to 1.371
VEGF	0,9717	0.203 to 1.74
ChM-I	-0,8333	-0.9336 to -0.7331
TSP1	0,535	-0.7466 to 1.817
ANGPTL4	-0,3938	-0.6827 to -0.1048

Figure 4. A-E
RM one way ANOVA (on raw data)

Variable	Mean Diff. (raw values)	95.00% CI of diff.
IL-34	2,955	0.8903 to 5.019
PTPRZ1	33,35	-0.7456 to 67.44
CSF1R	29,57	-19.71 to 78.86
IL-34 supernatant	0,3271	-0.02669 to 0.681
IL-34 Lysate	0,18	0.06573 to 0.2943

Figure 4. F-H
Paired t tests (on log transfo)

Variable	Mean of differences Hyp vs. Ctrl (log values)	95.00% CI of diff.
IL-34	0,6997	0.2273 to 1.172
IL-34 supernatant	1,488	0.8956 to 2.080
IL-34 Lysate	1,722	0.2740 to 3.171

Figure S4. A-D
Paired t tests (on log transfo)

Variable	Mean of differences Hyp vs. Ctrl (log values)	95.00% CI of diff.
SOX9	-0,4762	-0.8016 to -0.1508
ACAN	-0,2857	-0.4608 to -0.1105
MMP13	0,7034	-0.03504 to 1.442
TNAP	0,4004	-0.09972 to 0.9005

Figure 5. A

t-test with Welch correction (on raw data)

Variable	Mean of differences Hyp vs. Ctrl	95.00% CI of diff.
IL-34	264,9	23.43 to 506.4

Figure 6. A-G

RM one way ANOVA (on log transfo)

Variable	Mean Diff. (log values)	95.00% CI of diff.
CXCL12	0,06239	-0.01548 to 0.1403
CCL2	0,1648	-0.1723 to 0.5018
MMP3	-0,03512	-1.217 to 1.147
MMP13	-0,01926	-0.9422 to 0.9036
CCL2 prot	0,2363	-0.003122 to 0.4758
MMP3 prot	0,1776	-0.1418 to 0.497
MMP13 prot	0,03719	-0.1439 to 0.06955

Figure 7. A-I

RM one way ANOVA (on log transfo)

Variable	Mean Diff. (log values)	95.00% CI of diff.
CCL2	0,1863	-0.1877 to 0.5604
MMP3	0,8348	-0.3613 to 2.031
MMP13	0,9762	-0.3911 to 2.343
TNFA	0,6289	-0.6868 to 1.945
PEDF	0,02708	-0.07237 to 0.1265
PTPRZ1	-0,1447	-0.9248 to 0.6355
CCL2	0,1748	0.06643 to 0.2832
MMP3	0,1477	-0.055 to 0.3504
MMP13	0,07507	-0.01046 to 0.1606

ehyp vs. IMACs		
Fold-Changes	**Tukey's multiple comparisons test (Adjusted P Value)**	**Mean Diff. (raw values)**
-6,752	0,0001	-0,984
-9,524	0,0001	-0,9915
-3,469	0,0002	-0,84
-7,855	0,0001	-0,9625
10,109	0,0191	14,58
1,897	0,0969	-0,1228
3,098	0,0312	1,038
37,320	0,0441	33,28
2,559	0,0038	2,917
6,775	0,0232	9,678
2,245	0,1382	4,38
24,620	0,0527	23,54
8,807	0,0191	95,28
98,532	0,0435	4,462
1,140	0,0001	0,3642

s vs. Unstimulated		
Fold-Changes (back-transformed)	**Dunnett's multiple comparisons test (Adjusted P Value)**	**Mean Diff. (log values)**
-1,628	0,0454	-0,5062
-1,341	0,6357	-0,9513
64,565	0,0016	3,709
24,155	0,0045	1,065
1,307	0,532	0,7516
-1,177	0,8477	-1,269
-1,441	0,1184	-0,4658

Fold-Changes (back-transformed)	P values
22,210	0,0025
1,491	0,4523
1,014	0,948
1,120	0,5579
1,103	0,6786
2,382	0,0019
2,246	0,0001
22,550	0,0852
4,801	0,0008
8,730	0,0048
1,751	0,0241
1,972	0,0178
-5,999	0,0001
1,535	0,3779
-1,650	0,0146

ehyp vs. IMACs		
Fold-Changes	Tukey's multiple comparisons test (Adjusted P Value)	Mean Diff. (raw values)
3,955	0,0127	4,484
34,350	0,054	206,3
30,570	0,219	13,86
7,542	0,0667	0,24
5,320	0,0085	0,255

Fold-Changes (back-transformed)	P values
5,008	0,011
30,761	0,0013
52,723	0,0282

Fold-Changes (back-transformed)	P values
-2,994	0,0116
-1,931	0,0072
5,051	0,0586
2,514	0,0978

Fold-Change	P values
2,813	0,0368

3 vs. 0		
Fold-Changes (back-transformed)	Dunnett's multiple comparisons test (Adjusted P Value)	Mean Diff. (log values)
1,154	0,1091	0,001833
1,462	0,3721	0,1562
-1,084	0,9994	0,2485
-1,045	0,9997	0,2307
1,723	0,0526	0,1928
1,505	0,2886	0,025
1,089	0,6014	0,09637

3 vs. 0		
Fold-Changes (back-transformed)	Dunnett's multiple comparisons test (Adjusted P Value)	Mean Diff. (log values)
1,536	0,2973	0,1056
6,836	0,1399	0,7842
9,467	0,1319	0,804
4,255	0,3211	0,6068
1,064	0,6682	-0,1299
-1,395	0,8431	-0,4129
1,496	0,0098	0,2256
1,405	0,1251	0,1486
1,189	0,0743	0,08721

Hyp vs. IMACs			
95.00% CI of diff.	**Fold-Changes**	**Tukey's multiple comparisons test (Adjusted P Value)**	**Mean Diff. (raw values)**
-0.9861 to -0.9818	-62,500	0,0001	-0,1321
-1 to -0.9827	-117,647	0,0001	-0,09646
-1.003 to -0.6767	-6,250	0,0001	-0,1283
-0.971 to -0.9541	-26,667	0,0001	-0,08982
2.315 to 26.84	15,580	0,0266	5,467
-0.5728 to 0.3272	-1,140	0,6702	-1,02
0.522 to 1.555	2,038	0,0029	-1,06
20.98 to 45.58	34,280	0,0007	-3,039
2.269 to 3.564	3,917	0,0001	1,358
3.395 to 15.96	10,678	0,0094	3,903
0.5042 to 8.257	5,380	0,0322	3,135
-5.246 to 52.32	24,540	0,0964	-0,07917
40.94 to 149.6	96,280	0,0054	87,47
0.3415 to 8.583	98,751	0,0359	0,01019
0.2892 to 0.4391	8,026	0,0001	0,3569

Prehyp vs. Unstimulated			
95.00% CI of diff.	**Fold-Changes (back-transformed)**	**Dunnett's multiple comparisons test (Adjusted P Value)**	**Mean Diff. (log values)**
-0.685 to -0.3275	-3,208	0,0006	-0,7166
-1.624 to -0.2785	-8,939	0,0132	-0,6214
2.576 to 4.843	5116,818	0,0003	2,48
0.01016 to 2.12	11,614	0,0483	0,436
0.2524 to 1.251	5,644	0,0101	0,265
-1.749 to -0.7884	-18,578	0,0008	-0,9472
-0.8436 to -0.08814	-2,923	0,0229	-0,5362

Hyp vs. IMACs			
95.00% CI of diff.	**Fold-Changes**	**Tukey's multiple comparisons test (Adjusted P Value)**	**Mean Diff. (raw values)**
1.513 to 7.454	5,484	0,0102	1,529
85.4 to 327.2	207,300	0,006	172,9
-8.597 to 36.31	14,860	0,2053	-15,72
-0.003997 to 0.484	5,800	0,0532	-0,08714
0.1293 to 0.3807	7,120	0,0028	0,075

30 vs. 0			
95.00% CI of diff.	**Fold-Changes (back-transformed)**	**Dunnett's multiple comparisons test (Adjusted P Value)**	**Mean Diff. (log values)**
-0.1062 to 0.1099	1,004	0,9999	0,0797
-0.2005 to 0.5129	1,433	0,4473	0,2701
-0.5461 to 1.043	1,772	0,6682	0,1745
-0.7613 to 1.223	1,701	0,8153	0,3946
-0.05354 to 0.4391	1,559	0,1174	0,2639
-0.2209 to 0.2709	1,059	0,9775	0,1125
-0.2059 to 0.01311	1,248	0,0797	0,0881

30 vs. 0			
95.00% CI of diff.	**Fold-Changes (back-transformed)**	**Dunnett's multiple comparisons test (Adjusted P Value)**	**Mean Diff. (log values)**
-0.2305 to 0.4417	1,275	0,5837	0,2411
-0.5089 to 2.077	6,084	0,1967	0,6796
-0.7478 to 2.356	6,368	0,2754	0,7012
-0.721 to 1.935	4,044	0,3477	0,7616
-0.2301 to -0.02976	-1,349	0,0213	-0,1457
-0.9801 to 0.1544	-2,588	0,1254	-0,5416
0.07445 to 0.3767	1,681	0,013	0,4146
-0.02479 to 0.3219	1,408	0,0797	0,2832
0.01345 to 0.161	1,222	0,0291	0,1117

Hyp vs. Prehyp		
95.00% CI of diff.	**Fold-Changes**	**Tukey's multiple comparisons test (Adjusted P Value)**
-0.1697 to -0.09454	-9,256	0,0002
-0.1868 to -0.006102	-12,353	0,0396
-0.4144 to 0.1577	-1,802	0,383
-0.1302 to -0.04945	-3,395	0,0018
-11.71 to 22.64	1,541	0,5889
-2.136 to 0.09714	-2,162	0,068
-2.778 to 0.6579	-1,520	0,2054
-43.4 to 37.33	-1,089	0,9677
0.5405 to 2.175	1,531	0,0068
-6.132 to 13.94	1,576	0,4704
0.6722 to 5.598	2,396	0,0204
-41.74 to 41.58	-1,003	0,9999
34.33 to 140.6	10,932	0,007
-4.184 to 4.205	1,002	0,9999
0.2838 to 0.43	7,041	0,0001

Hyp vs. Unstimulated		
95.00% CI of diff.	**Fold-Changes (back-transformed)**	**Dunnett's multiple comparisons test (Adjusted P Value)**
-1.016 to -0.417	-5,207	0,0013
-1.018 to -0.2247	-4,182	0,0086
1.833 to 3.127	301,995	0,0002
0.08404 to 0.788	2,729	0,0225
0.04916 to 0.4809	1,841	0,0233
-1.324 to -0.5709	-8,855	0,001
-0.7502 to -0.3221	-3,437	0,001

Hyp vs. Prehyp		
95.00% CI of diff.	**Fold-Changes**	**Tukey's multiple comparisons test (Adjusted P Value)**
-0.3452 to 3.403	1,223	0,0971
82.31 to 263.6	6,035	0,0037
-54.35 to 22.91	-2,057	0,4429
-0.447 to 0.2727	-1,300	0,7486
-0.1534 to 0.3034	1,338	0,5711

100 vs. 0		
95.00% CI of diff.	**Fold-Changes (back-transformed)**	**Dunnett's multiple comparisons test (Adjusted P Value)**
-0.01186 to 0.1713	1,201	0,0828
-0.2201 to 0.7603	1,863	0,2944
-0.7296 to 1.079	1,495	0,8792
-0.4115 to 1.201	2,481	0,3712
-0.06649 to 0.5943	1,836	0,1101
-0.05553 to 0.2806	1,296	0,1846
-0.2153 to 0.03908	1,225	0,1684

100 vs. 0		
95.00% CI of diff.	**Fold-Changes (back-transformed)**	**Dunnett's multiple comparisons test (Adjusted P Value)**
-0.09881 to 0.581	1,742	0,1342
-1.051 to 2.411	4,782	0,4424
-1.26 to 2.662	5,026	0,5023
-0.472 to 1.995	5,776	0,1888
-0.2651 to -0.02623	-1,399	0,0262
-1.513 to 0.4296	-3,480	0,2367
0.2119 to 0.6174	2,598	0,0041
0.1544 to 0.4119	1,920	0,0031
0.06202 to 0.1614	1,293	0,0029